



Article

# Ouabain Enhances Cell-Cell Adhesion Mediated by $\beta_1$ Subunits of the $\text{Na}^+, \text{K}^+$ -ATPase in CHO Fibroblasts

Claudia Andrea Vilchis-Nestor<sup>1,2</sup>, María Luisa Roldán<sup>1</sup>, Angelina Leonardi<sup>3</sup>, Juan G. Navea<sup>3</sup> ,  
Teresita Padilla-Benavides<sup>2,\*</sup> and Liora Shoshani<sup>1,\*</sup>

<sup>1</sup> Department of Physiology Biophysics and Neurosciences, Center for Research and Advanced Studies, Cinvestav-Ipn, CDMX 07360, Mexico; cvilchis85@gmail.com (C.A.V.-N.); mroldan@fisio.cinvestav.mx (M.L.R.)

<sup>2</sup> Department of Biochemistry and Molecular Pharmacology, University of Massachusetts Medical School, Worcester, MA 01605, USA

<sup>3</sup> Department of Chemistry, Skidmore College, 815 North Broadway, Saratoga Springs, NY 12866, USA; aleonar1@skidmore.edu (A.L.); jnavea@skidmore.edu (J.G.N.)

\* Correspondence: terepadillabenavides@gmail.com (T.P.-B.); shoshani@fisio.cinvestav.mx (L.S.); Tel.: +1-508-856-5204 (T.P.-B.); +52-55-57-47-3360 (L.S.)

Received: 16 April 2019; Accepted: 26 April 2019; Published: 29 April 2019



**Abstract:** Adhesion is a crucial characteristic of epithelial cells to form barriers to pathogens and toxic substances from the environment. Epithelial cells attach to each other using intercellular junctions on the lateral membrane, including tight and adherent junctions, as well as the  $\text{Na}^+, \text{K}^+$ -ATPase. Our group has shown that non-adherent chinese hamster ovary (CHO) cells transfected with the canine  $\beta_1$  subunit become adhesive, and those homotypic interactions amongst  $\beta_1$  subunits of the  $\text{Na}^+, \text{K}^+$ -ATPase occur between neighboring epithelial cells. Ouabain, a cardiotonic steroid, binds to the  $\alpha$  subunit of the  $\text{Na}^+, \text{K}^+$ -ATPase, inhibits the pump activity and induces the detachment of epithelial cells when used at concentrations above 300 nM. At nanomolar non-inhibiting concentrations, ouabain affects the adhesive properties of epithelial cells by inducing the expression of cell adhesion molecules through the activation of signaling pathways associated with the  $\alpha$  subunit. In this study, we investigated whether the adhesion between  $\beta_1$  subunits was also affected by ouabain. We used CHO fibroblasts stably expressing the  $\beta_1$  subunit of the  $\text{Na}^+, \text{K}^+$ -ATPase (CHO  $\beta_1$ ), and studied the effect of ouabain on cell adhesion. Aggregation assays showed that ouabain increased the adhesion between CHO  $\beta_1$  cells. Immunofluorescence and biotinylation assays showed that ouabain (50 nM) increases the expression of the  $\beta_1$  subunit of the  $\text{Na}^+, \text{K}^+$ -ATPase at the cell membrane. We also examined the effect of ouabain on the activation of signaling pathways in CHO  $\beta_1$  cells, and their subsequent effect on cell adhesion. We found that cSrc is activated by ouabain and, therefore, that it likely regulates the adhesive properties of CHO  $\beta_1$  cells. Collectively, our findings suggest that the  $\beta_1$  subunit adhesion is modulated by the expression levels of the  $\text{Na}^+, \text{K}^+$ -ATPase at the plasma membrane, which is regulated by ouabain.

**Keywords:**  $\text{Na}^+, \text{K}^+$ -ATPase;  $\beta_1$  subunit; Ouabain; cSrc; pNaKtide; cell adhesion

## 1. Introduction

The  $\text{Na}^+, \text{K}^+$ -ATPase or sodium pump is an ubiquitous plasma membrane transporter that creates the ionic gradients that drive the net movement of glucose, amino acids, and ions across cellular membranes [1,2]. The  $\text{Na}^+, \text{K}^+$ -ATPase belongs to the P-type ATPase family, whose members are characterized by the transitory formation of a phosphorylated enzyme intermediate [3,4]. Structurally,

the pump consists of three subunits: a catalytic  $\alpha$  subunit, an accessory  $\beta$  subunit and a regulatory  $\gamma$  subunit. The catalytic  $\alpha$  subunit consists of 10 transmembrane domains (TM), and exchanges 3  $\text{Na}^+$  ions from the cytosol for 2  $\text{K}^+$  ions from the extracellular milieu using the energy released from ATP hydrolysis [5]. The  $\beta$  subunit is constituted by a single TM domain, and a long glycosylated extracellular domain. Its functions are discussed in detail below. The  $\gamma$  subunit is a small, single span TM protein belonging to the FXYD family, which is differentially expressed in tissues and modulates the pump's function [6,7]. In mammals, there are four  $\alpha$  subunit isoforms, three  $\beta$  subunit isoforms and seven FXYD members [2,8].

The  $\beta$  subunit of the sodium pump has different functions that depend on the isoform expressed ( $\beta_1$ ,  $\beta_2$  or  $\beta_3$ ), and on the accompanying  $\alpha$  subunit isoform ( $\alpha_1$ – $\alpha_4$ ) [9]. The main function of the  $\beta$  subunit is to act as a chaperone for the  $\alpha$  subunit, by contributing to the assembly and delivery of the pump to the plasma membrane [10,11]. In addition, the  $\beta$  subunit undergoes conformational changes during the catalytic cycle [12]. Different  $\beta$  isoforms have been associated with different  $\text{K}^+$  affinities [13]. Furthermore, some studies suggest that the  $\beta_1$  subunit regulates cell polarity, cell motility, epithelial to mesenchymal transition, and oncogenic transformation [14–16]. In epithelia, the  $\beta_1$  isoform functions as a homophilic cell adhesion molecule [17–19]. Moreover, the  $\beta_2$  isoform is an adhesion molecule on glia (AMOG, [20]).

Emerging evidence has shown that the  $\text{Na}^+, \text{K}^+$ -ATPase may have other regulatory functions in addition to pumping ions across cell membranes. Ouabain and other related cardiotonic steroids are highly specific  $\text{Na}^+, \text{K}^+$ -ATPase ligands that bind to all catalytic  $\alpha$  isoforms [21–23]. Studies from various laboratories have documented an important signaling function of the  $\text{Na}^+, \text{K}^+$ -ATPase [9,24]. In epithelia, the sodium pump also acts as a membrane receptor that transduces signals in response to ouabain and other related cardiotonic steroids. The binding of ouabain and cardiotonic steroids (at nM concentrations) to the sodium pump activates signaling pathways that resemble those triggered by hormone/receptor interactions, which, in turn, regulate gene expression, membrane trafficking, cell adhesion, proliferation, and cell death [25–30]. Interestingly, nanomolar concentrations of ouabain neither inhibit  $\text{K}^+$  pumping nor disturb the  $\text{K}^+$  balance of the cell [31]. Therefore, it was proposed that low ouabain concentrations bind and activate a non-pumping population of the  $\text{Na}^+, \text{K}^+$ -ATPase [32,33]. However, the nature of the effects that ouabain exerts at different concentrations in organisms is still controversial [34–36].

It was suggested that Ouabain is a hormone when Hamlyn and Mathews demonstrated the presence in plasma of a substance similar to ouabain in plants [22,37]. Thereafter, it was shown that endogenous ouabain is synthesized and secreted by the hypothalamus [38,39] and the adrenocortical gland [40–42]. The status of ouabain as a hormone was strengthened upon the discovery of increased concentrations in plasma during exercise, ingesting salty foods, and in pathological conditions such as arterial hypertension and myocardial infarction [43–48]. However, its physiological role remained unknown. Work from our group has shown that ouabain binding to the  $\text{Na}^+, \text{K}^+$ -ATPase modulates epithelial cell adhesion and communication [31,49,50].

Our laboratory has studied the role of the  $\text{Na}^+, \text{K}^+$ -ATPase  $\beta_1$  subunit in epithelia. We demonstrated that the  $\beta_1$  subunits of  $\text{Na}^+, \text{K}^+$ -ATPases on neighboring cells interact with each other in a species-specific manner [17,19]. Numerous studies have shown that the intercellular homotypic interaction between  $\beta_1$  subunits of the  $\text{Na}^+, \text{K}^+$ -ATPase are important for the stability of adherent junctions (AJ) and for the integrity of the tight junctions (TJ) [18,51]. Thus,  $\beta_1$ - $\beta_1$  interactions between epithelial cells are critical for the integrity of intercellular junctions. Since ouabain modulates different cell-attachment complexes, we wondered whether ouabain also regulates the  $\beta_1$ - $\beta_1$  mediated cell adhesion. In this work we used CHO fibroblasts, which lack the classical cell-cell adhesion complexes (TJs, AJ) and that stably express a canine  $\beta_1$  subunit in the plasma membrane. This model system targets the  $\text{Na}^+, \text{K}^+$ -ATPase efficiently to the plasma membrane contributing to the cell-cell contact [19]. To determine whether  $\beta_1$ - $\beta_1$  interactions are modulated by ouabain, we investigated the effect of a low dose (50 nM) of ouabain on the adhesion of CHO cells overexpressing the canine  $\beta_1$  subunit. This work shows that ouabain increases the

amount of  $\text{Na}^+,\text{K}^+$ -ATPase at the cell membrane, resulting in increased cell adhesion properties that are mediated by  $\beta_1$ - $\beta_1$  interactions. This effect is facilitated by the ouabain-dependent activation of kinases such as cSrc and AKT, which enhance the adhesive properties of CHO  $\beta_1$  cells.

## 2. Results

### 2.1. Cell-Cell Adhesion of CHO Fibroblasts Expressing Canine $\beta_1$ Subunit of $\text{Na}^+,\text{K}^+$ -ATPase is Mediated by $\beta_1$ Homotypic Interactions *in-trans*

Adherent CHO fibroblasts attach to the extracellular matrix and to their substrate, but establish weak cell-cell contacts, which are easily disrupted by gentle shaking or pipetting [19,52,53]. We have shown that CHO fibroblasts transfected with the canine  $\beta_1$  subunit of the  $\text{Na}^+,\text{K}^+$ -ATPase (CHO  $\beta_1$ ) form large cellular aggregates, due to an increase in cell-cell adhesion [19]. Moreover, we demonstrated that the epithelial  $\beta_1$  subunit of  $\text{Na}^+,\text{K}^+$ -ATPase is an adhesion molecule that mediates the interaction between sodium pumps on neighboring cells by establishing homotypic interactions [17]. Therefore, we hypothesized that the cell-cell adhesion observed in CHO  $\beta_1$  cells is mediated by  $\beta_1$ - $\beta_1$  interactions. To address this question, we investigated the subcellular localization of the canine  $\beta_1$  subunit and the cell-cell adhesion properties of CHO cells. Wild type CHO cells do not express the  $\beta_1$  subunit of the sodium pump (Figure 1A, left panel). Confocal microscopy analyses showed that CHO cells transfected with the plasmid encoding the canine  $\beta_1$  subunit express the protein in the plasma membrane, thereby showing a distribution resembling that observed in epithelial MDCK cells (Figure 1A, middle and right panels). Dispase assays showed that wild type CHO cells are unable to maintain cellular aggregates (Figure 1B, left panel). However, the cell-cell adhesion capability of CHO cells increased upon transfection of the canine  $\beta_1$  subunit similar to those of the CHO cells expressing the adhesion molecule E-cadherin, as these cells maintain larger cellular aggregates upon dispase disruption (CHO E-cadh; Figure 1B). On average, the aggregates formed by CHO  $\beta_1$  cells are significantly larger (3 fold) than control wild type CHO cells but similar in size to those observed in the CHO E-cadh cells (Figure 1C). Notably, CHO cells transfected with a plasmid encoding an irrelevant protein, the dopamine receptor 2 (CHO D2L, Figure 1 and Figure S1), failed to display adhesive properties similar to those of CHO  $\beta_1$  and CHO E-cadh cells (Figure 1B,C).

To confirm the hypothesis that the cell-cell adhesion observed in CHO  $\beta_1$  cells is due to  $\beta_1$ - $\beta_1$  interactions, we tested whether the soluble domain of the  $\beta_1$  subunit would impair the formation of cellular aggregates in this cell line. We took advantage of a truncated version of the canine  $\beta_1$  subunit that only expresses the soluble extracellular C-terminal domain (Sec $\beta_1$ ) [17,54]. CHO  $\beta_1$  cells were allowed to interact with supernatants obtained from CHO Sec $\beta_1$  cells containing this protein, and the formation of cellular aggregates was analyzed by light microscopy. Figure 1D shows that the presence of the soluble domain of the canine  $\beta_1$  subunit (Sec $\beta_1$ ) reduced the size of the CHO  $\beta_1$  cellular aggregates. Statistical analyses confirmed that the aggregates formed by CHO  $\beta_1$  cells were significantly smaller (~50%) than those formed by control cells (Figure 1E). Interestingly, confocal microscopy and cell quantification analyses showed that CHO  $\beta_1$  cells pre-incubated for 24 h with Sec $\beta_1$  supernatant presented a non-significant but consistent decrease in proliferation when compared to control cells (Figure 1D, lower panel, F). Remarkably, as can be observed in the IF images of Figure 1D (lower panel), contact naïve CHO  $\beta_1$  cells treated with Sec  $\beta_1$  unexpectedly express the  $\beta_1$  subunit at the plasma membrane and showed an intense and quantifiable fluorescence similar to the one observed in cell-cell contacts. These results confirmed that  $\text{Na}^+,\text{K}^+$ -ATPase- dependent cell-cell adhesion is at least partially due to an interaction between  $\beta_1$  subunits, and further showed that the cell culture model based on CHO  $\beta_1$  cells is suitable for studying  $\beta_1$ - $\beta_1$  interactions.

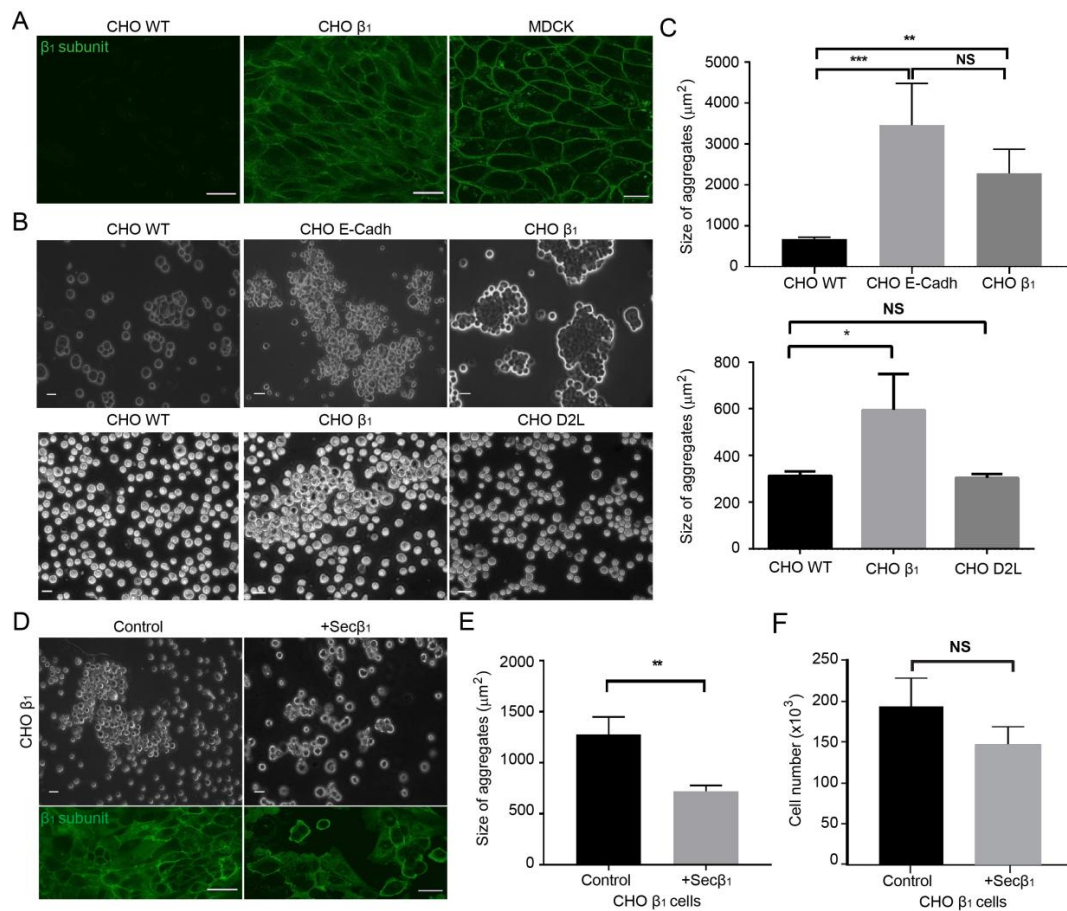


**Figure 1.** Cell-cell adhesion of CHO fibroblasts expressing the canine  $\beta_1$  subunit of  $\text{Na}^+,\text{K}^+$ -ATPase (CHO  $\beta_1$ ) is mediated by  $\beta_1$ - $\beta_1$  interactions. (A) Representative confocal microscopy images of CHO wild type, CHO  $\beta_1$  and MDCK cells immunostained against the canine  $\beta_1$  subunit. Scale bar = 30  $\mu\text{m}$ . (B) Representative light microscopy images of CHO wild type, CHO  $\beta_1$ , CHO E-Cadherin, and CHO D2L cells after the dispase aggregation assay. Scale bar = 20  $\mu\text{m}$ . (C) Quantification of the size of the aggregates is depicted as the area of their horizontal projections. Values represent the mean from three independent biological replicates  $\pm$  SE. Kruskal Wallis and Dunnet's t-test for multiple comparisons were performed; NS, non-significant, \*  $p < 0.05$ , \*\*  $p < 0.005$ , \*\*\*  $p < 0.0001$ . (D) Upper panels are representative phase-contrast micrographs of aggregation assays as in (B). Scale bar = 20  $\mu\text{m}$ . Lower panels are representative confocal microscopy images of the canine  $\beta_1$  subunit in CHO  $\beta_1$  cells incubated for 24 h in the absence (left) or presence (right) of Sec $\beta_1$ . (E) Quantification of the mean size of cellular aggregates of untreated CHO  $\beta_1$  cells or cells treated with Sec $\beta_1$ . Student t-test of three independent biological experiments  $\pm$  SD was performed; \*\*  $p < 0.005$ . (F) Proliferation assay of CHO  $\beta_1$  cells incubated for 24 h in the absence or presence of Sec $\beta_1$ . Student t-test of three independent biological experiments  $\pm$  SD was performed; NS, non-significant.

## 2.2. Ouabain Increases Cell-Cell Adhesion of CHO $\beta_1$ Cells

Nanomolar concentrations of ouabain modulate cell-cell interactions [29,31]. Therefore, we hypothesized that ouabain may also control the cell-cell interactions that are mediated by the  $\beta_1$  subunits of the sodium pump. To test this hypothesis, we used the dispase adhesion assay, to further investigate the adhesive properties of CHO  $\beta_1$  cells in the absence or presence of ouabain. Figure 2 shows a specific and significant increase of the size of CHO  $\beta_1$  cell aggregates upon treatment with ouabain at a concentration of 50 nM (compare Figure 2A upper and lower panels). Importantly, the inhibitory ouabain concentration (100  $\mu\text{M}$ ) decreased the cell adhesion phenotype observed in CHO  $\beta_1$  cells to that of wild type cells. Therefore, we concluded that low doses of ouabain (50 nM) increase

cell adhesion mediated by  $\beta_1$ - $\beta_1$  interactions of CHO  $\beta_1$  cells. Previous studies from our laboratory showed that the adhesive properties of CHO  $\beta_1$  cells do not involve the expression of adhesive proteins such as E-cadherin or  $\beta$ -catenin [19]. Consistent with this, we were unable to detect the expression of the adhesion markers  $\beta$ -catenin or E-cadherin in wild type and CHO  $\beta_1$  fibroblasts (Figure 2C). However, a small increase in the expression of p120 catenin was detected. Importantly, we utilized atomic absorbance spectroscopy (AAS) to evaluate the levels of  $\text{Na}^+$  and  $\text{K}^+$  in wild type and CHO  $\beta_1$  cells treated with 50 nM of ouabain. Figure 2D showed that the intracellular levels of  $\text{K}^+$  remained stable in untreated CHO wild type (CHO WT) and CHO  $\beta_1$  cells as well as in the fibroblasts treated with ouabain. The adhesive phenotype observed in the cells treated with a low dose of ouabain was specific to this cardiotonic steroid. Dispass assays and Western blot analyses showed that CHO  $\beta_1$  cells incubated with digoxin (50 and 100 nM) are unable to form cellular aggregates and that the induction of the  $\beta_1$  subunit does not occur with this cardiotonic steroid (Figure S2A,B). Furthermore, the intracellular levels of  $\text{K}^+$  in these cells also remained stable as shown by AAS analyses (Figure S2C). It is noteworthy that  $\text{Na}^+$  measurements by AAS were below the detection limit of this technique. All the samples tested had a  $\text{Na}^+$  concentration below 0.3 ppb in solution. Since no variations were detected between cells treated either with ouabain, or digoxin and non-treated cells, the data suggest that  $\text{Na}^+$  also remained stable in these cells.

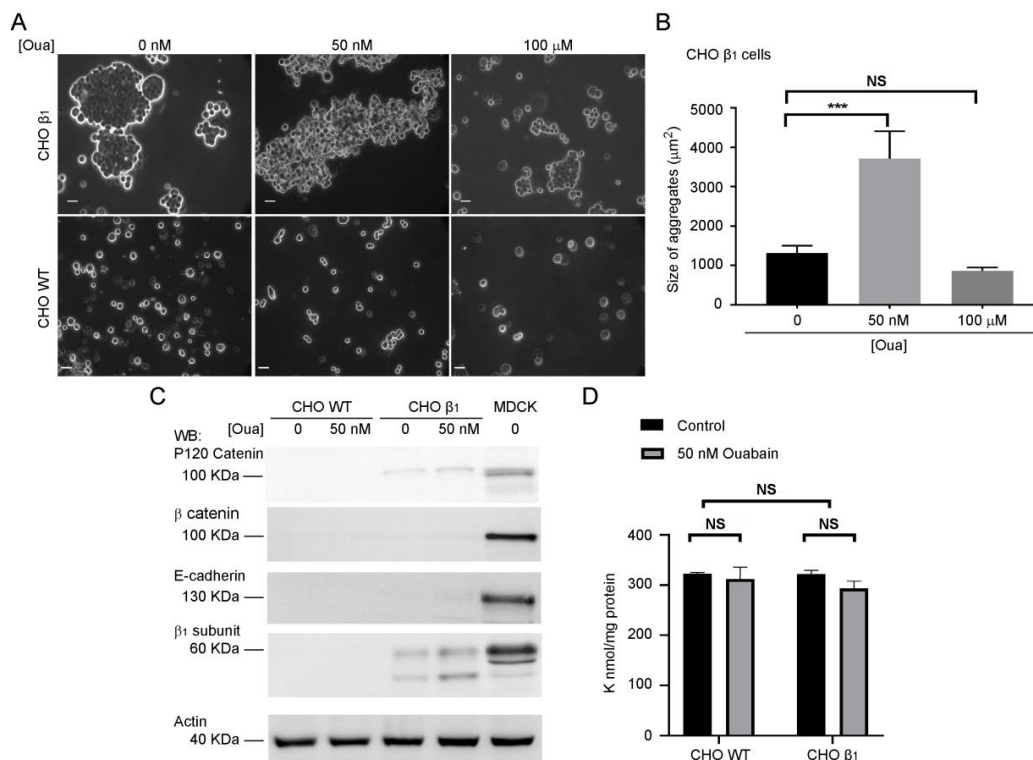


**Figure 2.** Low doses of ouabain increased cell-cell adhesion of CHO  $\beta_1$  cells. (A) Representative microscopy images of cell aggregation of CHO  $\beta_1$  cells (upper panels) and CHO WT cells (lower panels) treated with ouabain (50 nM, 100  $\mu\text{M}$ ). Scale bar = 20  $\mu\text{m}$ . (B) Quantification of the mean size of cellular aggregates of CHO  $\beta_1$  cells treated with 0, 50 nM and 100  $\mu\text{M}$  ouabain based on three independent biological replicates. One way ANOVA and Dunn's tests for multiple comparison were performed. Bars represent  $\pm$  SE; NS, non-significant, \*\*\*  $p < 0.0001$ . (C) Representative Western blot analyses of the adhesion markers p120 catenin,  $\beta$  catenin, E-cadherin, and the  $\beta_1$  subunit of the sodium pump in CHO  $\beta_1$  and CHO WT cells, untreated or treated with 50 nM of ouabain. MDCK cells were used as positive control. Actin was used as loading control. (D) Whole cell content of  $\text{K}^+$  was determined by AAS from CHO  $\beta_1$  and CHO WT cells treated with 50 nM of ouabain for 24 h. The average of three independent biological replicates is depicted. One-way ANOVA and Dunn's tests for multiple comparison were performed, bars represent  $\pm$  SE, NS, non-significant.

### 2.3. The Interactions of $\beta_1$ - $\beta_1$ Subunits are Stable *in vitro* Independently of Ouabain Treatment

The effect of ouabain on cell-cell interactions mediated by  $\beta_1$  subunits could be due to the induction of a conformational change in  $\beta_1$  subunits by this cardiotonic steroid, resulting in a more adhesive molecule. Accordingly, ouabain binding to its receptor, the  $\alpha$  subunit of the pump, should be sufficient for inducing the same effect on  $\beta_1$ - $\beta_1$  interactions *in vitro*. Therefore, we studied whether ouabain directly affects  $\beta_1$ - $\beta_1$  subunits interaction in a pull-down assay. In this case, we used the canine  $\beta_1$  tagged with a hexa-histidine repeat (CHO  $\beta_1$  6His) immobilized on Ni<sup>+</sup>-NTA as the bait. The prey was obtained from total cellular extract of CHO  $\beta_1$  cells tagged with the yellow fluorescent protein (CHO  $\beta_1$  YFP). CHO WT cells were used as negative control. Cellular extracts (bait and prey) were allowed to interact in the absence or presence of ouabain, and the formation of the interacting  $\beta_1$  subunit complexes were analyzed by Western blot. Figure 3 shows that the immobilized CHO  $\beta_1$  6His was able to interact with the recombinant  $\beta_1$  YFP obtained from cellular extracts. Importantly, the interaction *in vitro* was maintained, even in the presence of ouabain (Figure 3A). Statistical analyses demonstrated that ouabain treatment did not affect the amount of interacting proteins significantly (Figure 3B). All eluted fractions contained the  $\alpha$  subunit, which means that the  $\beta_1$  6His is assembled with the  $\alpha$  subunit on the Ni<sup>+</sup>-NTA beads (Figure 3A). The data suggest that the effect of ouabain on cell-adhesion does not occur directly on  $\beta_1$  subunits, and that it is likely dependent on additional cellular components.

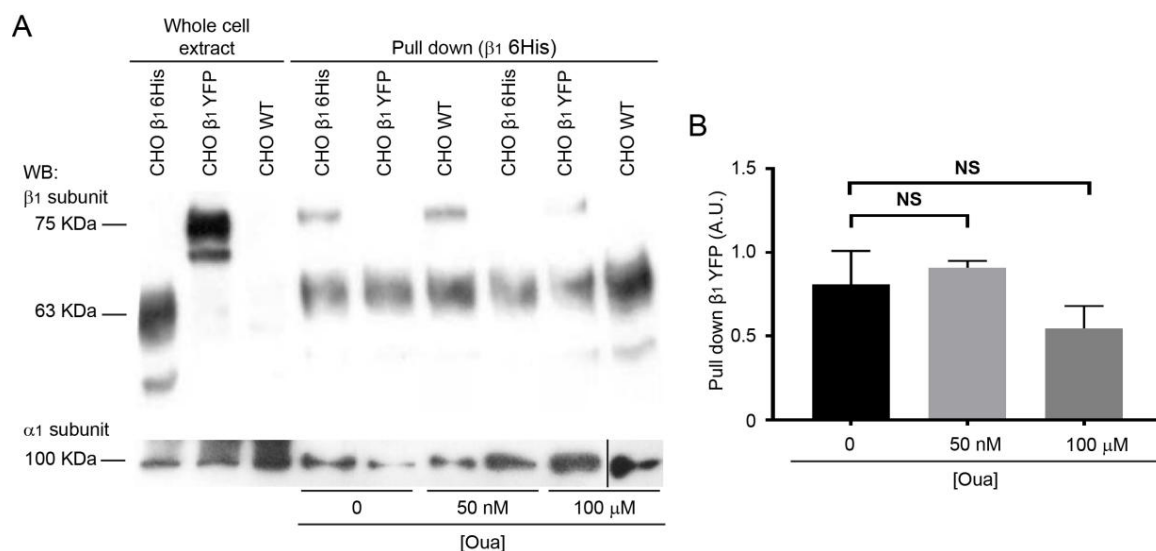


**Figure 3.** A direct interaction between ouabain and the  $\alpha_1$  subunit of Na<sup>+</sup>,K<sup>+</sup>-ATPase is not sufficient for the observed adhesive phenotype. (A) Western blot analysis of  $\beta_1$  and  $\alpha_1$  subunits of the Na<sup>+</sup>,K<sup>+</sup>-ATPase: cell lysate of CHO  $\beta_1$  6His, CHO  $\beta_1$  YFP and CHO WT cells (three left lanes); Pull Down assay between CHO  $\beta_1$  6His as a bait and CHO  $\beta_1$  YFP or CHO WT as a prey with 0 nM, 50 nM and 100  $\mu$ M Ouabain (six right lanes). The 63 KDa band corresponds to the  $\beta_1$  6His, and the higher-molecular-weight band corresponds to the  $\beta_1$  YFP (75 KDa), both recognized by the same anti- $\beta_1$  subunit antibody. (B) Densitometric quantification of the results presented in A. In pulled down fractions, the density of the  $\beta_1$  YFP band was normalized with the  $\beta_1$  6His band. Data represent the mean of three independent replicates. Kruskal Wallis and Dunn's test for multiple comparisons were performed. Error bars,  $\pm$  SE; NS, non-significant.

### 2.4. Ouabain Increases the Expression and Localization of the Sodium Pump at the Plasma Membrane

It has been shown that treatment with cardiotonic steroids (ouabain and 21-benzylidene digoxin) increases the expression levels of the  $\alpha$  subunit of sodium pumps in the porcine and canine kidney epithelium cell lines (LLC-PK1 and MDCK respectively) [55,56]. Therefore, we investigated whether the enhancing effect of ouabain on cell adhesion in CHO  $\beta_1$  cells was due to an increase in the

expression of the sodium pump at the plasma membrane. As expected, treatment of MDCK cells with ouabain at nanomolar concentrations (10–50 nM) increased the expression of the  $\beta_1$  subunit at the plasma membrane (Figure 4A), which is in agreement with the observations of Rocha and coworkers (2014) [56]. On the other hand, treatment with ouabain at  $\mu$ M concentrations leads to the detachment of the MDCK cells (Figure 4A; [57]). Considering these phenotypes, we evaluated the effect of ouabain on the localization of the  $\beta_1$  subunit in the monolayer of CHO  $\beta_1$  cells. Confocal microscopy analyses showed that in our model system, the  $\beta_1$  subunit has a similar distribution in CHO cells to that in epithelial cells upon ouabain treatment (Figure 4B). In addition, the membrane localization of the sodium pump is disrupted at higher concentrations of ouabain ( $\mu$ M) (Figure 4B). Notably, the fluorescence intensity of the  $\beta_1$  subunit at the plasma membrane only increased significantly upon treatment with 50 nM ouabain (Figure 4C).

To confirm that nanomolar concentrations of ouabain increase the sodium pump expression at the plasma membrane, we used a surface biotinylation assay. Figure 4D shows a representative Western blot analysis of the  $\beta_1$  subunit located in the plasma membrane of CHO  $\beta_1$  cells treated with 50 nM ouabain. Statistical analyses of three independent biological experiments showed a small but significant increase in the membrane expression of the  $\beta_1$  subunit in CHO  $\beta_1$  cells (Figure 4D,E). Our results suggest that the observed increase in cell adhesion mediated by  $\beta_1$  subunits is a result of ouabain binding to the  $\alpha$  subunit, which may lead to the activation of signaling pathways that promote the expression and delivery of the pump to the plasma membrane.

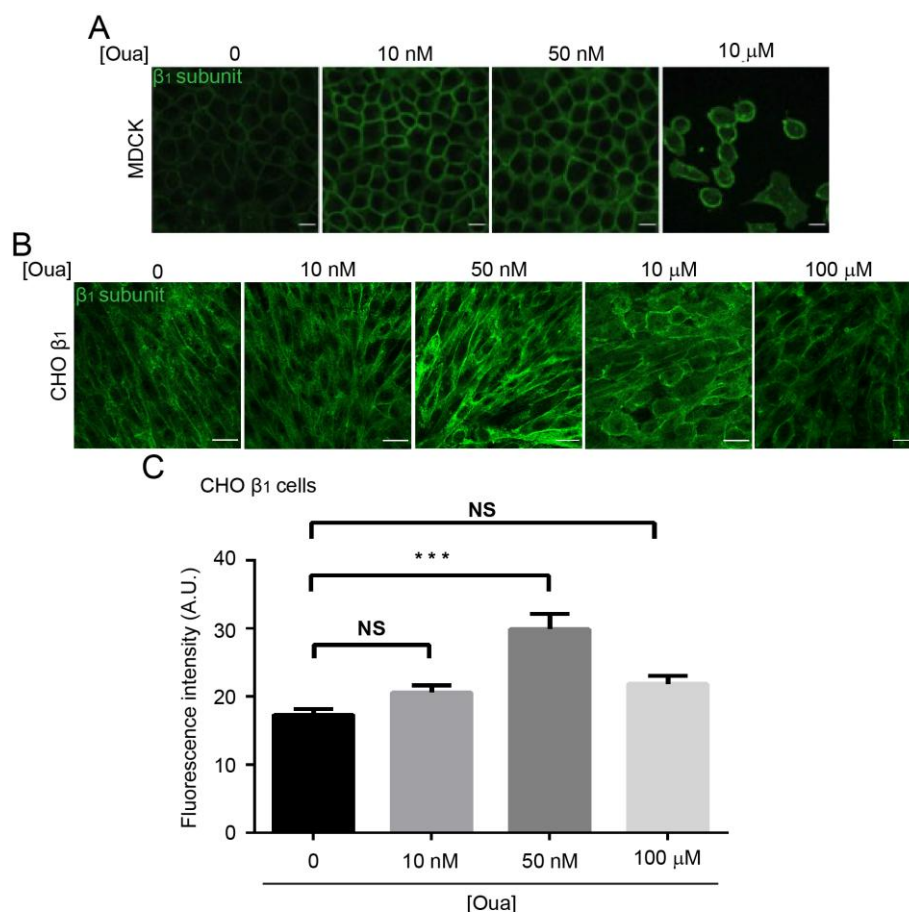
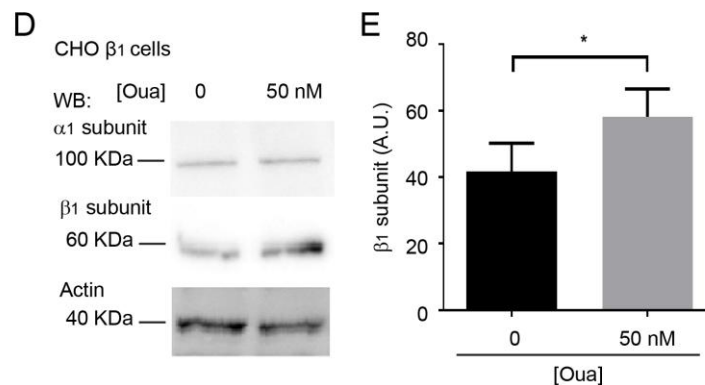


Figure 4. Cont.



**Figure 4.** Ouabain increases the expression of the  $\text{Na}^+, \text{K}^+$ -ATPase at the plasma membrane of CHO fibroblasts transfected with the canine  $\beta_1$  subunit. (A) Representative confocal microscopy images of the canine  $\beta_1$  subunit in MDCK cells incubated with 10, 50 nM and 10  $\mu\text{M}$  of Ouabain for 24 h, scale bar = 20  $\mu\text{m}$ . (B) Representative confocal microscopy images of the canine  $\beta_1$  subunit in CHO  $\beta_1$  cells incubated for 24 h with 10, 50 nM, 10, and 100  $\mu\text{M}$  of ouabain, scale bar = 20  $\mu\text{m}$ . (C) Quantification of the fluorescence intensity observed at the plasma membrane of CHO  $\beta_1$  cells (10 cells per field of three independent biological replicates). One way ANOVA and Dunn's test for multiple comparisons were performed. The data represent the mean  $\pm$  SE; NS, non-significant, \*\*\*  $p < 0.0001$ . (D) Representative Western blot analysis of  $\beta_1$  and  $\alpha_1$  subunits of the  $\text{Na}^+, \text{K}^+$ -ATPase of CHO  $\beta_1$  cells biotinylated after treatment with 50 nM ouabain for 24 h. Actin was used as a loading control for the input of the corresponding samples. (E) Densitometry quantification of biotinylated  $\beta_1$  subunit after treatment with ouabain. The data represent the mean of three independent biological replicates  $\pm$  SD, Student t-test was performed; \*  $p < 0.05$ .

### 2.5. The $\beta_1$ - $\beta_1$ Adhesion Enhanced by Ouabain Depends on the Activation of cSrc and AKT Signaling Pathway

Previous studies demonstrated that binding of cardiotonic steroids such as ouabain to the sodium pump stimulates multiple kinase cascades [58]. Therefore, the effect of ouabain on the  $\beta_1$ - $\beta_1$  interaction could be explained by the potential activation of some components from the signaling machinery that are known to modulate cell junctions such as TJs, AJs and GAP junctions [31,59]. We first screened for signaling proteins of the tyrosine kinase family that were differentially activated in CHO  $\beta_1$  and CHO WT cells. Overall, CHO  $\beta_1$  cells had more active signaling proteins than wild type cells, indicating that the increased expression of  $\text{Na}^+, \text{K}^+$ -ATPase in CHO fibroblasts induces the activation of signaling cascades that usually have low activity (Figure S3). Then, we treated CHO  $\beta_1$  cells with 50 nM ouabain and identified various kinases that were altered when treating the ouabain cells (Figure S4). Of all the modified pathways detected, we focused on the potential mechanisms by which cSrc, AKT, and ERK1/2 contribute to the interaction between the  $\beta_1$  subunits. We selected these kinases, as they have been extensively reported by our group and others, to participate in cell adhesion and migration processes [49,60–65]. Western blot and quantitative band analyses from the three kinases selected showed that phosphorylated cSrc and AKT increased significantly upon treatment with 50 nM ouabain compared to control cells (Figure 5A). No significant phosphorylation effect of ERK1/2 was detected upon addition of ouabain (Figure 5A). The effect on kinase activation was also specific to ouabain, as treatment with digoxin failed to induce this effect (Figure S5). Then, we investigated whether the inhibition of those pathways would impair the effect of ouabain on cell adhesion mediated by  $\beta_1$  subunits. The selected phosphorylation inhibitors were Dasatinib for cSrc, Perifosine for AKT, and U01266 for ERK1/2. The incubation of the CHO  $\beta_1$  cells with all the inhibitors was effective and prevented the corresponding kinase phosphorylation in the presence or absence of ouabain (Figure 5A). Therefore, to test the effect of kinase inhibition on the ouabain-dependent adhesive properties of CHO  $\beta_1$  cells, we analyzed the size of the cellular aggregates. Representative light microscopy imaging showed that inhibition of cSrc and AKT impaired the enhanced ouabain-dependent formation of cellular aggregates (Figure 5B). No changes in the size of CHO  $\beta_1$  cellular aggregates in which ERK1/2

was inhibited were observed (Figure 5B). Statistical analyses showed significant differences in the size of CHO  $\beta_1$  cell aggregates treated with either perifosine or dasatinib; no significant differences were observed in CHO  $\beta_1$  cells treated with U0126 compared to control cells (Figure 5C). These results suggest that ouabain binding to the sodium pump stimulates cSrc kinase and AKT signaling pathways, which may be involved in the regulation of  $\beta_1$ - $\beta_1$  mediated cell adhesion.

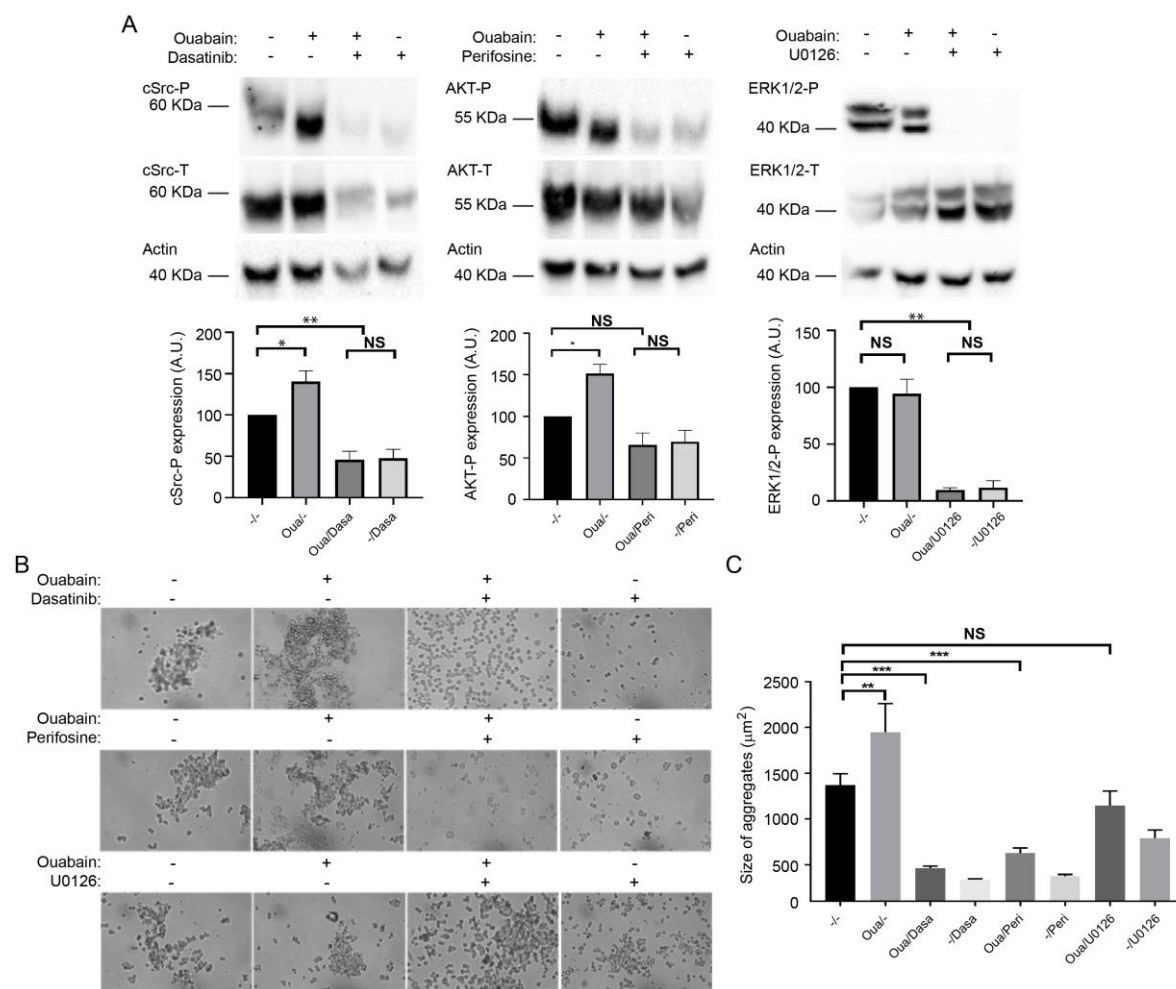


**Figure 5.** Src and AKT signaling pathways are involved in ouabain modulation of cell-cell adhesion of CHO  $\beta_1$  fibroblasts. (A) Representative Western blot analysis (upper panel) and quantification (lower panel) of cSrc-P, AKT-P, and ERK1/2-P of non treated (-) CHO  $\beta_1$  cells, and independent cultures treated with 50 nM ouabain (+), and in the presence (+) or absence (-) of the specific kinase inhibitor: cSrc (Dasatinib, 100 nM); AKT (Perifosine, 10  $\mu\text{M}$ ); and EKR1/2 (U0126, 10  $\mu\text{M}$ ) ( $n = 3$ ). The inhibitors were added 1 h prior to incubation with ouabain for 60 min. NS, non-significant, \*  $p < 0.05$ , \*\*  $p < 0.005$ . (B) Representative images of dispase aggregation assay of untreated control (-/-) CHO  $\beta_1$  and cells treated with 50 nM ouabain and the specific inhibitors for cSrc, Dasatinib; AKT, Perifosine; and EKR1/2, U0126. Image taken at a magnification 5 $\times$ . (C) Quantification of the size of cellular aggregates. The data represent the mean of three independent biological replicates  $\pm$  SE. Kruskal Wallis and Dunn's test for multiple comparisons were performed. NS, non-significant, \*\*  $p < 0.005$ , \*\*\*  $p < 0.0001$ .

### 2.6. pNaKtide Reduces Cell Adhesion Effect Exerted by Ouabain

The  $\text{Na}^+, \text{K}^+$ -ATPase interacts with cSrc kinase and forms a complex that serves as a receptor for ouabain to stimulate various protein kinase cascades [33]. Specifically, ouabain binding to the  $\text{Na}^+, \text{K}^+$ -ATPase disrupts this interaction and results in the assembly and activation of different signaling pathways [66]. Thus far, our results have shown that the adhesive properties of  $\beta_1$  subunits require the

cellular context, since no effect of ouabain was observed *in vitro* (Figure 3). Moreover, the increased phosphorylation of cSrc in CHO  $\beta_1$  cells treated with ouabain (Figure 5A), was reverted by the cSrc kinase inhibitor, and prevented formation of cellular aggregates (Figure 5B,C). Therefore, we hypothesized that the ouabain-dependent  $\beta_1$  subunit adhesive properties could be partially due to the activation of the  $\text{Na}^+, \text{K}^+$ -ATPase/cSrc complex. To test this hypothesis we took advantage of the pNaKtide, which is a peptide that antagonizes the effect of ouabain on cSrc [67], and assayed for cell-adhesion in the presence of ouabain with or without the pNaKtide. Figure 6A shows a representative Western blot of the ouabain-dependent increase in the phosphorylation of cSrc (~70% higher than control cells). In the presence of 1  $\mu\text{M}$  of the pNaKtide, the effect on cSrc phosphorylation was abolished, and remained at similar levels to control cells. No changes were detected in the expression of the  $\alpha$  subunit of the sodium pump. Finally, we analyzed the effect of the antagonist on the formation of ouabain-dependent aggregates of CHO  $\beta_1$  cells. Representative light microscopy images showed that the size of the antagonist-treated cell aggregates is smaller compared to the ouabain stimulated cells (Figure 6B). Statistical analyses showed that, in the presence of the pNaKtide, the size of ouabain-stimulated aggregates is similar to that of control cells (Figure 6C). These results support our hypothesis that the adhesion effect of  $\beta_1$  subunits stimulated by ouabain is partially regulated by cSrc activation.

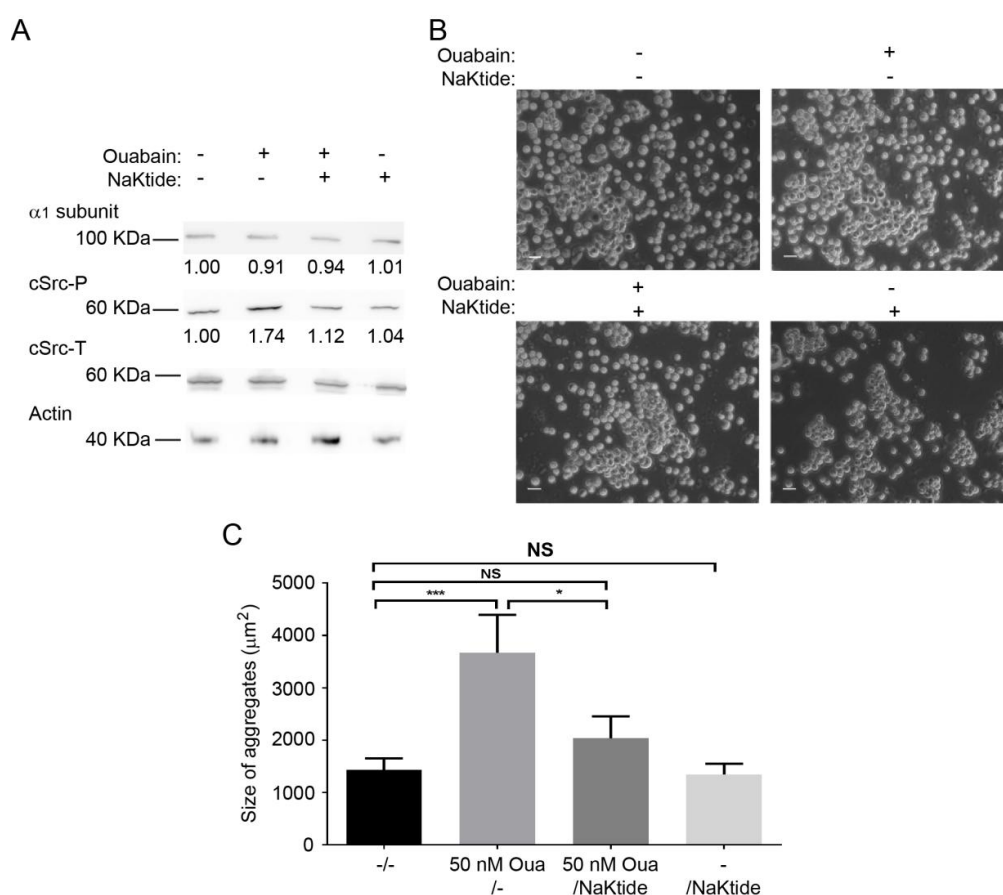


**Figure 6.** pNaKtide inhibits Ouabain-activated cSrc and ouabain enhanced  $\beta_1$ -mediated cell adhesion in CHO  $\beta_1$  cells. (A) Representative Western blot of cSrc activation (cSrcP), total cSrc (cSrcT), and  $\alpha_1$  subunits of CHO  $\beta_1$  cells treated with (+) or without (−) 50 nM ouabain and 1  $\mu\text{M}$  pNaKtide for 24 h ( $n = 3$ ). Actin was used as loading control. (B) Representative microscopy images of the disperse assay of CHO  $\beta_1$  cells treated with (+) or without (−) 50 nM ouabain and 1  $\mu\text{M}$  pNaKtide for 24 h; scale bar = 20  $\mu\text{m}$ . (C) Quantification of the size of cellular aggregates of CHO  $\beta_1$  control non-treated cells (−/−), and CHO  $\beta_1$  cells cultured with (+) or without (−) 50 nM ouabain and 1  $\mu\text{M}$  pNaKtide. The data represent the mean of three independent biological replicates  $\pm$  SE. Kruskal Wallis and Dunn’s test for multiple comparisons were performed. NS non-significant, \*  $p < 0.05$ , \*\*\*  $p < 0.0001$ .

### 3. Discussion

As all mammalian cells, CHO fibroblasts express the necessary amount of sodium pumps at their plasma membrane for maintaining a suitable ionic balance that maintains their viability. In our overexpression system, the assembled  $\alpha_1\beta_1$  dimer in CHO  $\beta_1$  cells is targeted to the plasma membrane and concentrated at cell-cell contacts, thereby leading to the adoption of an epithelial-like phenotype and to the maintenance of both cell-cell and cell-substrate adhesion [19]. This phenotype makes the CHO  $\beta_1$  overexpression system an ideal model to investigate cell adhesion. Our group has demonstrated previously that the  $\beta_1$  subunits of neighboring cells can interact directly in a species-specific manner by using the cellular system and biochemical tools described in this study [17]. We show that increasing the density of the  $\beta_1$  subunit of the  $\text{Na}^+$ -pump in cell contacts of CHO fibroblasts is sufficient for displaying a cell-adhesive phenotype. These adhesive properties are mediated by  $\beta_1$  interactions, which are regulated by signaling cascades that ensure the establishment and maintenance of classical epithelial adhesion complexes [29,31,50].

Early work from the Nelson group on epithelial cell polarity showed that expression of E-cadherin in L-fibroblasts, which lack surface polarity, resulted in membrane domains with apical and basolateral identities [68]. Remarkably, the endogenous  $\text{Na}^+$ -pumps in those experiments were recruited to cell-cell contacts. Our results show that CHO fibroblasts transfected with the  $\beta_1$  subunit, a  $\text{Ca}^{2+}$ -independent adhesion molecule, or with E-cadherin, a  $\text{Ca}^{2+}$ -dependent cell adhesion molecule, display similar aggregation properties. Moreover, overexpression of an irrelevant membrane protein, the Dopamine receptor D2L, did not induce cell-cell aggregation. Nevertheless, overexpression of  $\beta_1$  subunit in CHO cells does not induce the expression of classical adhesion markers such as E-cadherin and  $\beta$  catenin. Curiously, p120 catenin was detected by Western blot in CHO  $\beta_1$  cells, but not in WT cells. This observation could be related to the apparent “epithelialization” of the CHO  $\beta_1$  cells. To validate that cell-cell adhesion of CHO  $\beta_1$  cells was in fact due to  $\beta_1$ - $\beta_1$  interactions, cellular aggregation was challenged with Sec $\beta_1$ , the soluble extra-cellular domain of the canine  $\beta_1$  subunit. As expected, this truncated version of the  $\beta_1$  prevented the cell-cell adhesion properties observed in CHO  $\beta_1$  cells. These results strongly suggest that Sec $\beta_1$  competes for cell-cell adhesion mediated by  $\beta_1$  subunits on neighboring cells and that the effect of ouabain on cell-cell adhesion is indeed through  $\beta_1$ - $\beta_1$  interactions. Remarkably, Sec $\beta_1$  blocks cell-cell aggregation between CHO  $\beta_1$  cells only when it is added shortly after seeding and before the formation of a confluent monolayer. This observation indicates that Sec $\beta_1$  is not able to compete with formed  $\beta_1$ - $\beta_1$  interactions but can interact with non-occupied  $\beta_1$  subunit and to prevent cell-cell adhesion mediated by  $\beta_1$  subunits. Moreover, CHO  $\beta_1$  cells pre-incubated with Sec $\beta_1$  do not reach confluence, but rather form small patches or are observed as single cells. We wondered whether this was due to a proliferation defect. Our results show that the Sec $\beta_1$  treated cells indeed tend to proliferate less than the untreated ones. Usually, contact naïve epithelial cells do not express the  $\text{Na}^+$ -pump at the plasma membrane [69]. Notably, MDCK cells co-cultured with CHO WT cells do not express the  $\text{Na}^+, \text{K}^+$ -ATPase at the heterotypic contacting membrane [19]. Nevertheless, some of the CHO  $\beta_1$  single cells showed a highly fluorescent signal at the plasma membrane, which corresponded to the  $\beta_1$  subunit. Therefore, it is plausible that these contact naïve CHO  $\beta_1$  cells are actually surrounded by soluble Sec $\beta_1$  molecules associated with the membrane-bound  $\beta_1$  subunit, thereby mimicking cell-cell contacts. As such, we hypothesize that the apparent proliferation defect is due to contact inhibition induced by Sec  $\beta_1$ . These results lead to a new paradigm of the sodium pump- dependent modulation of cell proliferation. Altogether, these results confirm that cell-cell adhesion of CHO fibroblasts that overexpress  $\text{Na}^+, \text{K}^+$ -ATPase is mainly based on  $\beta_1$ - $\beta_1$  interactions between neighboring cells.

Ouabain binding to the  $\alpha$  subunit of the epithelial  $\text{Na}^+, \text{K}^+$ -ATPase has a dual effect on the pump, whereby high concentrations of ouabain (>300 nM) trigger pump inhibition and cell detachment [49,57]. Low concentrations of ouabain increase sodium pump activity [70,71], and stimulate cellular signaling pathways [30]. In epithelial MDCK cells, ouabain concentrations between 10 and 100 nM are known to modulate cell contacts, such as TJs, AJs and GAP junctions [29,31,49,50]. We analyzed the effect of

ouabain on the effect of  $\beta_1$ - $\beta_1$  mediated cell adhesion. Our results show that CHO  $\beta_1$  cells incubated with low concentrations of ouabain (50 nM) did not have altered  $K^+$  concentrations. However, this low dose allows the formation of bigger aggregates than those observed in non-treated cells. On the other hand, incubation with high concentration of ouabain (100  $\mu$ M) partially prevented the cell-cell adhesion effect observed in CHO  $\beta_1$  cells. Since these cells remain partially adhesive, we cannot overrule the possibility of an effect of ouabain that is independent of the  $\beta_1$  subunit although we could not detect classical cell-adhesion markers such as E-cadherin and  $\beta$ -catenin in control or ouabain treated CHO  $\beta_1$  cells. Therefore, our results strongly suggest that low concentrations of ouabain induce an increase in  $\beta_1$ - $\beta_1$  interaction in CHO  $\beta_1$  cells.

We then asked whether ouabain had a direct effect on the  $\beta_1$ - $\beta_1$  interaction. Ouabain binding to the  $\alpha$  subunit could induce a localized conformational change that would make the  $\beta_1$  subunit more adhesive which could be considered a direct effect. Ouabain binding produces conformational rearrangements in the  $\alpha$  subunit of the sodium pump [72]. Furthermore, fluorometry assays identified three positions on the  $\beta_1$  subunit, that indicate that  $\alpha$  and  $\beta$  subunits move toward each other during conformational transition and produce a conformational rearrangement [12,73]. To further assess this process, our in vitro experiments showed that although the  $\alpha$  subunit is present during the immobilization on Ni-NTA and pull down assays, ouabain treatment does not modify  $\beta_1$ - $\beta_1$  interaction. As such, our results suggest that ouabain does not modify the adhesion between  $\beta_1$  subunits directly and that it requires additional cellular components to fulfill this function. In this regard, binding of ouabain to the  $\alpha$  subunit could activate signaling cascades that would up-regulate the amount of  $Na^+,K^+$ -ATPase exposed to the extracellular space and thus indirectly increase cell-cell adhesion mediated by  $\beta_1$  subunits. It was established that epithelial cells express at least two different populations of the  $Na^+,K^+$ -ATPases: A pumping population and a signaling (non-pumping) population [25,66,74,75], which could be the case for transfected CHO  $\beta_1$  fibroblasts. Overexpression of the  $\beta_1$  subunit up-regulates the expression of the  $\alpha$  subunit [32,76]. Both are assembled in the endoplasmic reticulum and targeted to the plasma membrane [77]. Consistent with this idea, confocal microscopy and surface biotinylation analyses performed in this study showed that ouabain stimulates the expression and delivery of the pump to the plasma membrane. Apparently, the signaling population is increased because we observed that, even without ouabain, the basal expression of cSrc, AKT, and ERK1/2 is increased in comparison to non-transfected CHO cells. Studies are now directed to understand the participation of the  $\beta_1$  subunit in the activation of additional signaling cascades in a ouabain-independent fashion (shown in Figure S3), and are beyond the scope of this manuscript. Moreover, nanomolar concentrations of ouabain stimulated the activation of cSrc; furthermore, the pNaKtide, which only binds to cSrc associated with  $Na^+,K^+$ -ATPase, successfully reverted the effect of ouabain on cSrc activation and cell-cell adhesion. Importantly, a fundamental difference between digoxin and ouabain is the apparent failure of digoxin to activate Src kinase [78]. This feature may explain the observed lack of an adhesive effect of digoxin. In addition, AKT seems to regulate the ouabain-dependent cell-cell adhesion observed in CHO  $\beta_1$  fibroblasts, as the specific inhibitor of AKT abolished the  $\beta_1$ -mediated cell-cell adhesion. This is not surprising, as it has been shown that AKT trans-activates IP3K, which forms part of the signaling complex in association with  $Na^+,K^+$ -ATPase [28,79]. On the other hand, the inhibition of ERK signaling cascade had a minor effect on the ouabain-dependent cellular aggregation. This might be partially explained by the fact that ERK1/2 is not the only signaling effector activated by cSrc [80,81]. Moreover, our initial screening revealed various signaling proteins that were not further analyzed and that could be involved, such as TrkB, EphB4 and PDGFR. Future studies will focus on understanding the role of these signaling molecules in the  $\beta_1$ - $\beta_1$  adhesion phenotype.

All together, our results suggest that overexpression of the  $\beta_1$  subunit in CHO cells increases the population of  $Na^+,K^+$ -ATPases at the plasma membrane. This pool of pumps is most probably involved in mediating  $\beta_1$ - $\beta_1$  interactions between neighboring cells. Whether these proteins have an active role in ion transport remains to be elucidated, but considering the data obtained by AAS, it is unlikely that the role of these pumps is limited to ion transport. A plausible model could involve

the activation of cSrc and AKT upon stimulation of CHO  $\beta_1$  cells with nanomolar concentrations of ouabain. These signaling cascades would result in the overexpression of adherent pumps targeted to cell contacts at the plasma membrane. Nonetheless, an open question that would have to be addressed in the future is if CHO  $\beta_1$  cells form signalosomes as epithelial cells do, and if  $\beta_1$ - $\beta_1$  interactions occur between specific pools (pumping and non-pumping pool). This study highlights the importance of the  $\beta_1$  subunit of the  $\text{Na}^+, \text{K}^+$ -ATPase and strengthens the new paradigm that this subunit of the sodium pump is a novel drug target to prevent cancer metastasis, where the deregulation of cell adhesion is a major detrimental pathological effect.

#### 4. Materials and Methods

##### 4.1. Cell Culture

Starter Cell lines, MDCK (Madin-Darby Canine Kidney, CCL-34) and CHO-K1 (Chinese hamster ovary) were obtained from the American Type Culture Collection. CHO-K1 cells were cultured in a mixture of F12/DMEM (1132-082, Invitrogen, Carlsbad, CA, USA), supplemented with 10% fetal calf serum (FCS) (200-6170, Invitrogen), 100 U/mL penicillin, and 100  $\mu\text{g}/\text{mL}$  streptomycin (600-5145, Invitrogen) and MDCK cells were cultured in DMEM (430-1600, Invitrogen) supplemented with 10% FCS (200-6170, Invitrogen), 100 U/mL penicillin, and 100  $\mu\text{g}/\text{mL}$  streptomycin (600-5145, Invitrogen). Cells were grown at 36.5 °C a 5%  $\text{CO}_2$  atmosphere, 90% humidity (Forma Scientific  $\text{CO}_2$  incubator, Steri-Cult 200).

For all experiments, the cells were depleted of serum 24 h before adding different concentrations of ouabain (3125, Sigma-Aldrich, St. Louis, MO, USA), or digoxin (458350, Tocris Bioscience, Bristol, UK) as indicated in the figures (10 nM, 50 nM, 100 nM 10  $\mu\text{M}$  or 100  $\mu\text{M}$ ).

CHO-K1 cells were transfected with pCIN4- $\beta_1$  (CHO  $\beta_1$ ), pIRESneo-6His (CHO  $\beta_1$  6His), and the canine pEYFP- $\beta_1$  (CHO  $\beta_1$  YFP) plasmids as previously described [17,19,51]. CHO-K1 cells transfected with EcDendra [82] were a kind gift of Dr. P. Nava (Cinvestav, Mexico). CHO-K1 cells expressing the dopamine receptor 2 (CHO D2L, pcDNA3.1 D2L) were a kind gift of Dr. J. A. Arias-Montaña (Cinvestav, Mexico) The construct for secreted ecto-domain of the canine  $\beta_1$  subunit (Sec $\beta_1$ ) was a kind gift of Dr. D. M. Fambrough (Johns Hopkins University, USA), and was generated as previously reported [83]. Sec $\beta_1$  was transfected in CHO cells as described by Padilla-Benavides, et al., 2010 [17]. CHO Sec $\beta_1$  cells were cultured in serum free media for 4 days before collecting the conditioned medium containing the ecto-domain of  $\beta_1$  subunit [17,54]. Stable clones were selected and maintained with 0.2 mg/mL G418 (11811031, Thermo Fischer Scientific, Waltham, MA, USA) in F12/DMEM mixture.

For experiments including Sec $\beta_1$  the CHO  $\beta_1$  cells were seeded in 24 wells plates and after 90 min the monolayer was washed three times with PBS and a serum free medium with or without Sec $\beta_1$  was added. The next day the medium was replaced with a medium containing ouabain and Sec $\beta_1$ .

The kinase inhibitors used were against cSrc (Dasatinib 100 nM), AKT (Perifosine 10  $\mu\text{M}$ ), ERK1/2 (U0126, 10  $\mu\text{M}$ ) (0952, 14,240 and 9903, respectively, Cell Signaling Technologies, Danvers, MA, USA) and pNaKtide (1  $\mu\text{M}$ ) was a kind gift of Dr. Z. Xie (Marshall Institute for Interdisciplinary Research, USA). Inhibitors were added 1 h before ouabain treatment.

##### 4.2. Antibodies

The primary antibodies used were: mouse anti- $\alpha_1$ -subunit of the  $\text{Na}^+, \text{K}^+$ -ATPase (7671, Abcam, Cambridge, UK). Mouse anti- $\beta_1$ -subunit of the  $\text{Na}^+, \text{K}^+$ -ATPase (kind gift of Dr. M. Caplan, Yale University, USA). Rabbit anti-phospho-Akt (Ser473, D9E), rabbit anti-phospho-p44/42 MAPK (Erk1/2, Thr202/Tyr204, D13.14.4E); rabbit anti-phospho-Src Family (Tyr416, D49G4); rabbit anti-Akt (pan, C67E7); rabbit anti-p44/42 MAPK (Erk1/2, 137F5), and rabbit anti-Src (36D10) (4060, 4370, 6943, 4691, 4695, and 2109, respectively, Cell Signaling Technologies) The following rabbit antibodies were obtained from Abclonal (Woburn, MA, USA): anti-Src total (A0324), anti-p120 catenin (A1641), anti- $\beta$  catenin

(A11343), anti-E cadherin (A3044), anti-phospho-Src-Y416 (AP0480), anti-ERK1/ERK2 total (A16686), anti-phospho-ERK1-T202/Y204 and ERK2-T185/Y187 (AP0472).

The secondary antibodies used were: goat anti-rabbit IgG, and goat anti-mouse IgG coupled to HRP (65-6120 and 62-6520, respectively, Thermo Fisher Scientific). Goat anti-mouse IgG Alexa 488-conjugated (A11094, Molecular Probes, Eugene, OR, USA).

#### 4.3. Immunofluorescence and Confocal Microscopy Analyses

CHO and MDCK cells grown on coverslips at the indicated conditions in the figures, were immunostained as previously described [19]. Briefly, the cells were washed with PBS, fixed and permeabilized with ice-cold methanol for 5 min. After washing with PBS, the cells were blocked with 3% bovine serum albumin for 1 h, followed by 1 h incubation with a mouse primary antibody against the  $\beta_1$  subunit of the  $\text{Na}^+, \text{K}^+$ -ATPase (1:50 dilution) at room temperature. Cells were washed 10 times quickly with PBS, and incubated with a goat anti-mouse Alexa 488 secondary antibody (1:500 dilution) for 30 min at room temperature. After washing, the cells were mounted on glass slides with FluoroGuard antifade reagent (170–3140, BioRad, Hercules, CA, USA). Samples were imaged using a confocal microscope (Leica TCS SP8, Leica, Wetzlar, Germany), and visualized using the Leica Lite software. The relative fluorescence intensity was quantified using IMAGEJ Fiji 1.0 software [84].

#### 4.4. Western Blot Analysis

Monolayers of CHO cells grown on multi-well plates were washed 3 times with ice-cold PBS and incubated in RIPA buffer (24948A, Santa Cruz Biotechnologies, Dallas, TX, USA) with protease inhibitors (2498, Santa Cruz) for 30 min under continuous and vigorous shaking. After that the cells were scraped and collected into a 1.5 mL microcentrifuge tube. The cell extract was homogenized with insulin syringe and centrifuged at  $17,700 \times g$  for 10 min. The supernatant was recovered, and protein concentration was quantified by BCA as indicated by the manufacturer (23225, Pierce Chemical Co. Dallas, TX, USA). Thirty  $\mu\text{g}$  of protein were separated on 10% SDS-PAGE gels, electro-transferred onto a PVDF membrane (RPN 303F, Hybond-P Amersham Biosciences, Little Chalfont, UK), and detected using the indicated primary (anti- $\alpha_1$ -subunit of the  $\text{Na}^+, \text{K}^+$ -ATPase (1:2000), mouse anti- $\beta_1$ -subunit of the  $\text{Na}^+, \text{K}^+$ -ATPase (1:500). The rabbit anti-phospho-Akt, anti-phospho-p44/42 MAPK, anti-phospho-Src, anti-Akt, anti-p44/42 MAPK, anti-Src, anti-E cadherin, anti- $\beta$  catenin and anti-p120 catenin were used at a 1:2000 dilution. The appropriate secondary antibodies (goat anti-rabbit IgG, and goat anti-mouse IgG coupled to HRP and goat anti-mouse IgG Alexa 488-conjugated were used at a 1:10,000 dilution. Membranes were developed with ECL PLUS (RPN2132, Amersham Biosciences). Immunoblots were imaged by FUSIONFX (Vilber, Marne-la-Vallée, France) and ChemiDocXRS (BioRad), and quantified by densitometry using the IMAGEJ, Fiji 1.0 software [84].

#### 4.5. Cell Surface Biotinylation

Confluent monolayers of CHO  $\beta_1$  cells were depleted of serum for 24 h and then incubated with or without 50 nM ouabain for 24 h. Then, the monolayers were washed 3 times with PBS, and incubated with 1 mg/mL of EZ-Link Sulfo-NHS-SS-Biotin (21331, Thermo Fischer Scientific) for 30 min. Subsequently the monolayers were washed 3 times with PBS containing 100 mM glycine to quench the excess of Biotin, followed by a final wash with PBS containing 1% Triton X-100 and protease inhibitors. After 30 min, the cells were scraped, and the cell lysate collected into a 1.5 mL microcentrifuge tubes. The extract was homogenized by passing it 10 times through insulin syringe and centrifuged for 10 min at  $9000 \times g$  at  $4^\circ\text{C}$ . The supernatant was recovered, and the protein content was measured using the BCA protein assay method. The biotinylated extracts were incubated overnight at  $4^\circ\text{C}$  with 100  $\mu\text{L}$  of streptavidin-agarose suspension (S1638, Sigma-Aldrich). The next day, bead-adherent complexes were washed 5 times with PBS, and finally the proteins were eluted in  $2 \times$  Laemmli buffer and boiling for 5 min.

#### 4.6. Cell Adhesion Assay (Dispase Assay)

Confluent Monolayers of CHO  $\beta_1$  cells seeded on 24 well plates were depleted of serum for 24 h, and then incubated with or without ouabain (50 nM) for 24 h. Then the monolayers were washed with ice-cold PBS, and detached from the plates by incubation with PBS without  $\text{Ca}^{2+}$  supplemented with 0.6 U/mL of Dispase I (D4818, Sigma-Aldrich) for 35 min at 37 °C. Subsequently the Dispase solution was carefully removed using a 200  $\mu\text{L}$  pipette tip, and replaced by 100  $\mu\text{L}$  of PBS. The cells were then mechanically stressed by pipetting up and down 5 times using a 200  $\mu\text{L}$  pipette. The resulting aggregates were visualized by light microscopy using the 10  $\times$  and 20  $\times$  objectives (Axiovert 200M Fluorescence/Live Cell Imaging, Carl Zeiss, Oberkochen, Germany). Three independent biological replicates were imaged using the AxioVision 4.8 software. The number of aggregates was counted using the Fiji 1.0 software cell counter (aggregates < 200  $\mu\text{m}^2$  were excluded from the quantification) [84].

#### 4.7. Pull Down Assay (PD)

Total extract of CHO cells expressing the  $\beta_1$  6His construct were immobilized with nickel-nitrilotriacetic acid beads ( $\text{Ni}^{2+}$ -NTA, His Trap FF column; GE Healthcare, Chicago, IL, USA) equilibrated with 10 mL of RIPA buffer containing protease inhibitors. Total protein extracts (500  $\mu\text{g}$ ) were loaded into the resin, and allowed to interact for 3 h at 4 °C with gentle shaking. Then the unbound protein was washed as indicated by the manufacturer, and the total extract of CHO  $\beta_1$  YFP cells incubated in the presence or absence of ouabain (50 nM and 100  $\mu\text{M}$ ) were loaded as a prey. Samples were incubated overnight at 4 °C, and washed with PBS supplemented with 10 and 20 mM imidazole. Interacting proteins were eluted in PBS containing 500 mM imidazole and were analyzed by Western blot.

#### 4.8. Whole Cell $\text{K}^+$ and $\text{Na}^+$ Determinations by Atomic Absorbance Spectroscopy

The analysis of both potassium and sodium concentrations from cells obtained from 15  $\text{cm}^2$  plates was carried out by at least triplicate measurements using atomic absorption spectroscopy (AAS) equipped with a graphite furnace (GF-AAS) (AAAnalyst 800, PerkinElmer, Waltham, MA, USA) with hollow cathode lamps as the radiation source [85–87]. In order to reach the lowest possible limit of detection and eliminate possible contamination, the graphite tubes used were cleaned via high-temperature gas-phase procedures (UltraClean THGA Graphite Tubes, PerkinElmer). This technique allows trace elemental analysis at a relative low cost in low volume samples, where dilution can be limited by the low initial concentration of analyte in the sample. A known mass of sample was acid digested in concentrated  $\text{HNO}_3$ , using a single-stage digestion method [86–89]. To avoid contamination in the trace elemental analysis, all reagents used for sample treatment and calibration standard preparation were analytical grade and, when appropriate, diluted in 18 M $\Omega$  purified water. All analytical glassware was acid washed overnight in 10% (*v/v*) HCl and rinsed with 18 M $\Omega$  purified water before used.

Sodium and potassium standard solutions (1000 mg/L from Sigma-Aldrich) were diluted to obtain appropriate standards and determine the limits of detection and dynamic range of the method. The limit of detection (LOD) for K and Na, calculated as  $3\sigma$ , was 0.1 ppb and 0.3 ppb, respectively. The dynamic range for K and Na span from their LOD to a maximum concentration of 150 ppb and 200 ppb, respectively. Sodium and potassium content on each sample was normalized to the initial protein concentration of cells.

#### 4.9. Statistical Analysis

GraphPad Prism version 7.00 software (San Diego, CA, USA) was used for all statistical analyses. The data are presented, as the mean  $\pm$  SEM or SD as indicated in the figures. Statistical significance was determined using ANOVA one way and Kruskal Wallis test, and *t*-test for two conditions.  $p \leq 0.05$  was considered significant.

## 5. Conclusions

Research has shown that the homotypic interactions between  $\beta_1$  subunits of the  $\text{Na}^+, \text{K}^+$ -ATPase contributes to the stability and integrity of AJs and TJs in epithelial cells. In addition, the cardiotonic steroid ouabain further modulates various cell-attachment complexes. The work presented here demonstrated that ouabain also regulates cellular adhesion mediated by  $\beta_1$ - $\beta_1$  subunits. We showed that the presence of  $\beta_1$  subunits of the  $\text{Na}^+, \text{K}^+$ -ATPase at the cell surface promotes cellular contacts, and these interactions were further enhanced by low doses of ouabain. The activation of ouabain-dependent kinases such as cSrc and AKT, are responsible for the increased adhesive properties observed in CHO  $\beta_1$  cells, which ultimately contribute to the establishment of a broader adhesive phenotype in cells.

**Supplementary Materials:** Supplementary Materials can be found at <http://www.mdpi.com/1422-0067/20/9/2111/s1>.

**Author Contributions:** Conceptualization, L.S., T.P.-B. and C.A.V.-N.; methodology, C.A.V.-N., M.L.R., T.P.-B., J.G.N. and L.S.; investigation, C.A.V.-N., M.L.R., J.G.N., A.L. and T.P.-B.; resources, L.S. and T.P.-B.; writing—original draft preparation, C.A.V.-N., L.S. and M.L.R.; writing—review and editing, L.S., T.P.-B., C.A.V.-N. and J.G.N.; supervision, L.S. and T.P.-B.; project administration, L.S.; funding acquisition, L.S. and T.P.-B.

**Funding:** This research was funded by research grant (L.S.) and research fellowship (C.A.V.-N.) from CONACYT (National Research Council of México, grant number 127460), and by the Faculty Diversity Scholars Award from the University of Massachusetts Medical School, to T.P.-B.

**Acknowledgments:** The authors thank Xie Z. for the pNaKtide; to P. Nava, J. A. Arias-Montaña and D. M. Fambrough for providing constructs and cell lines. We also thank Rosalia Aguirre and Pablo Reyes-Gutierrez for their dedicated technical assistance, and to Ruben G. Contreras for all the useful discussions and comments on the manuscript. We are also thankful to Lyne Khair, Amanda L. Paskavitz and Daniel Hidalgo for their contributions to the final edition of this manuscript.

**Conflicts of Interest:** The authors declare no conflict of interest. The funding sponsors had no role in the design of the study; in the collection, analyses, or interpretation of data; in the writing of the manuscript, and in the decision to publish the results.

## References

1. Skou, J.C. The influence of some cations on an adenosine triphosphatase from peripheral nerves. *Biochim. Biophys. Acta* **1957**, *23*, 394–401. [[CrossRef](#)]
2. Blanco, G.; Mercer, R.W. Isozymes of the Na-K-atpase: Heterogeneity in structure, diversity in function. *Am. J. Physiol.* **1998**, *275*, F633–F650.
3. Post, R.L.; Sen, A.K.; Rosenthal, A.S. A phosphorylated intermediate in adenosine triphosphate-dependent sodium and potassium transport across kidney membranes. *J. Biol. Chem.* **1965**, *240*, 1437–1445.
4. Pedersen, P.L.; Carafoli, E. Ion motive atpases. I. Obiquity, properties, and significance to cell function. *Trends Biochem. Sci.* **1987**, *12*, 146–150.
5. Post, R.L.; Hegyvary, C.; Kume, S. Activation by adenosine triphosphate in the phosphorylation kinetics of sodium and potassium ion transport adenosine triphosphatase. *J. Biol. Chem.* **1972**, *247*, 6530–6540.
6. Therien, A.G.; Blostein, R. Mechanisms of sodium pump regulation. *Am. J. Physiol. Cell Physiol.* **2000**, *279*, C541–C566. [[CrossRef](#)]
7. Morth, J.P.; Pedersen, B.P.; Toustrup-Jensen, M.S.; Sorensen, T.L.; Petersen, J.; Andersen, J.P.; Vilsen, B.; Nissen, P. Crystal structure of the sodium-potassium pump. *Nature* **2007**, *450*, 1043–1049. [[CrossRef](#)] [[PubMed](#)]
8. Geering, K. Functional roles of Na,K-atpase subunits. *Curr. Opin. Nephrol. Hypertens.* **2008**, *17*, 526–532. [[CrossRef](#)] [[PubMed](#)]
9. Bagrov, A.Y.; Shapiro, J.I.; Fedorova, O.V. Endogenous cardiotonic steroids: Physiology, pharmacology, and novel therapeutic targets. *Pharmacol. Rev.* **2009**, *61*, 9–38. [[CrossRef](#)] [[PubMed](#)]
10. Chow, D.C.; Forte, J.G. Functional significance of the beta-subunit for heterodimeric p-type atpases. *J. Exp. Biol.* **1995**, *198*, 1–17.
11. Geering, K. The functional role of beta subunits in oligomeric p-type atpases. *J. Bioenerg. Biomembr.* **2001**, *33*, 425–438. [[CrossRef](#)] [[PubMed](#)]

12. Dempski, R.E.; Friedrich, T.; Bamberg, E. The beta subunit of the Na<sup>+</sup>/K<sup>+</sup>-atpase follows the conformational state of the holoenzyme. *J. Gen. Physiol.* **2005**, *125*, 505–520. [[CrossRef](#)] [[PubMed](#)]
13. Crambert, G.; Hasler, U.; Beggah, A.T.; Yu, C.; Modyanov, N.N.; Horisberger, J.D.; Lelievre, L.; Geering, K. Transport and pharmacological properties of nine different human Na,K-atpase isozymes. *J. Biol. Chem.* **2000**, *275*, 1976–1986. [[CrossRef](#)] [[PubMed](#)]
14. Rajasekaran, S.A.; Palmer, L.G.; Quan, K.; Harper, J.F.; Ball, W.J., Jr.; Bander, N.H.; Peralta Soler, A.; Rajasekaran, A.K. Na,K-atpase beta-subunit is required for epithelial polarization, suppression of invasion, and cell motility. *Mol. Biol. Cell* **2001**, *12*, 279–295. [[CrossRef](#)]
15. Espineda, C.E.; Chang, J.H.; Twiss, J.; Rajasekaran, S.A.; Rajasekaran, A.K. Repression of Na,K-atpase beta1-subunit by the transcription factor snail in carcinoma. *Mol. Biol. Cell* **2004**, *15*, 1364–1373. [[CrossRef](#)]
16. Madan, P.; Rose, K.; Watson, A.J. Na/K-atpase beta1 subunit expression is required for blastocyst formation and normal assembly of trophectoderm tight junction-associated proteins. *J. Biol. Chem.* **2007**, *282*, 12127–12134. [[CrossRef](#)]
17. Padilla-Benavides, T.; Roldan, M.L.; Larre, I.; Flores-Benitez, D.; Villegas-Sepulveda, N.; Contreras, R.G.; Cereijido, M.; Shoshani, L. The polarized distribution of Na<sup>+</sup>,K<sup>+</sup>-atpase: Role of the interaction between {beta} subunits. *Mol. Biol. Cell* **2010**, *21*, 2217–2225. [[CrossRef](#)]
18. Tokhtaeva, E.; Sachs, G.; Souda, P.; Bassilian, S.; Whitelegge, J.P.; Shoshani, L.; Vagin, O. Epithelial junctions depend on intercellular trans-interactions between the Na,K-atpase beta(1) subunits. *J. Biol. Chem.* **2011**, *286*, 25801–25812. [[CrossRef](#)]
19. Shoshani, L.; Contreras, R.G.; Roldan, M.L.; Moreno, J.; Lazaro, A.; Balda, M.S.; Matter, K.; Cereijido, M. The polarized expression of Na<sup>+</sup>,K<sup>+</sup>-atpase in epithelia depends on the association between beta-subunits located in neighboring cells. *Mol. Biol. Cell* **2005**, *16*, 1071–1081. [[CrossRef](#)]
20. Gloor, S.; Antonicek, H.; Sweadner, K.J.; Pagliusi, S.; Frank, R.; Moos, M.; Schachner, M. The adhesion molecule on glia (amog) is a homologue of the beta subunit of the Na,K-atpase. *J. Cell Biol.* **1990**, *110*, 165–174. [[CrossRef](#)]
21. Askari, A.; Kakar, S.S.; Huang, W.H. Ligand binding sites of the ouabain-complexed (Na<sup>+</sup> + K<sup>+</sup>)-atpase. *J. Biol. Chem.* **1988**, *263*, 235–242. [[PubMed](#)]
22. Hamlyn, J.M.; Blaustein, M.P.; Bova, S.; DuCharme, D.W.; Harris, D.W.; Mandel, F.; Mathews, W.R.; Ludens, J.H. Identification and characterization of a ouabain-like compound from human plasma. *Proc. Natl. Acad. Sci. USA* **1991**, *88*, 6259–6263. [[CrossRef](#)] [[PubMed](#)]
23. Laursen, M.; Gregersen, J.L.; Yatime, L.; Nissen, P.; Fedosova, N.U. Structures and characterization of digoxin- and bufalin-bound Na<sup>+</sup>,K<sup>+</sup>-atpase compared with the ouabain-bound complex. *Proc. Natl. Acad. Sci. USA* **2015**, *112*, 1755–1760. [[CrossRef](#)]
24. Aizman, O.; Uhlen, P.; Lal, M.; Brismar, H.; Aperia, A. Ouabain, a steroid hormone that signals with slow calcium oscillations. *Proc. Natl. Acad. Sci. USA* **2001**, *98*, 13420–13424. [[CrossRef](#)]
25. Haas, M.; Askari, A.; Xie, Z. Involvement of src and epidermal growth factor receptor in the signal-transducing function of Na<sup>+</sup>,K<sup>+</sup>-atpase. *J. Biol. Chem.* **2000**, *275*, 27832–27837. [[CrossRef](#)] [[PubMed](#)]
26. Li, J.; Zelenin, S.; Aperia, A.; Aizman, O. Low doses of ouabain protect from serum deprivation-triggered apoptosis and stimulate kidney cell proliferation via activation of nf-kappab. *J. Am. Soc. Nephrol.* **2006**, *17*, 1848–1857. [[CrossRef](#)]
27. Liu, J.; Liang, M.; Liu, L.; Malhotra, D.; Xie, Z.; Shapiro, J.I. Ouabain-induced endocytosis of the plasmalemmal Na/K-atpase in llc-pk1 cells requires caveolin-1. *Kidney Int.* **2005**, *67*, 1844–1854. [[CrossRef](#)]
28. Liu, L.; Zhao, X.; Pierre, S.V.; Askari, A. Association of pi3k-akt signaling pathway with digitalis-induced hypertrophy of cardiac myocytes. *Am. J. Physiol. Cell Physiol.* **2007**, *293*, C1489–C1497. [[CrossRef](#)] [[PubMed](#)]
29. Larre, I.; Cereijido, M. Na,K-atpase is the putative membrane receptor of hormone ouabain. *Commun. Integr. Biol.* **2010**, *3*, 625–628. [[CrossRef](#)] [[PubMed](#)]
30. Tian, J.; Li, X.; Liang, M.; Liu, L.; Xie, J.X.; Ye, Q.; Kometiani, P.; Tillekeratne, M.; Jin, R.; Xie, Z. Changes in sodium pump expression dictate the effects of ouabain on cell growth. *J. Biol. Chem.* **2009**, *284*, 14921–14929. [[CrossRef](#)]
31. Larre, I.; Lazaro, A.; Contreras, R.G.; Balda, M.S.; Matter, K.; Flores-Maldonado, C.; Ponce, A.; Flores-Benitez, D.; Rincon-Heredia, R.; Padilla-Benavides, T.; et al. Ouabain modulates epithelial cell tight junction. *Proc. Natl. Acad. Sci. USA* **2010**, *107*, 11387–11392. [[CrossRef](#)]

32. Liang, M.; Tian, J.; Liu, L.; Pierre, S.; Liu, J.; Shapiro, J.; Xie, Z.J. Identification of a pool of non-pumping Na/K-ATPase. *J. Biol. Chem.* **2007**, *282*, 10585–10593. [[CrossRef](#)]
33. Tian, J.; Cai, T.; Yuan, Z.; Wang, H.; Liu, L.; Haas, M.; Maksimova, E.; Huang, X.Y.; Xie, Z.J. Binding of src to Na<sup>+</sup>,K<sup>+</sup>-ATPase forms a functional signaling complex. *Mol. Biol. Cell* **2006**, *17*, 317–326. [[CrossRef](#)]
34. Simonini, M.; Casanova, P.; Citterio, L.; Messaggio, E.; Lanzani, C.; Manunta, P. Endogenous ouabain and related genes in the transition from hypertension to renal diseases. *Int. J. Mol. Sci.* **2018**, *19*, 1948. [[CrossRef](#)]
35. Simonini, M.; Casanova, P.; Citterio, L.; Messaggio, E.; Lanzani, C.; Manunta, P. Reply: “Comment on: Endogenous ouabain and related genes in the transition from hypertension to renal diseases”. *Int. J. Mol. Sci.* **2019**, *20*, 542. [[CrossRef](#)]
36. Furstenwerth, H. Comment on: Endogenous ouabain and related genes in the transition from hypertension to renal diseases, *Int. J. Mol. Sci.* **2018**, *19*, 1948. *Int. J. Mol. Sci.* **2019**, *20*, 505. [[CrossRef](#)]
37. Mathews, W.R.; DuCharme, D.W.; Hamlyn, J.M.; Harris, D.W.; Mandel, F.; Clark, M.A.; Ludens, J.H. Mass spectral characterization of an endogenous digitalis-like factor from human plasma. *Hypertension* **1991**, *17*, 930–935. [[CrossRef](#)]
38. Ludens, J.H.; Clark, M.A.; DuCharme, D.W.; Harris, D.W.; Lutzke, B.S.; Mandel, F.; Mathews, W.R.; Sutter, D.M.; Hamlyn, J.M. Purification of an endogenous digitalis-like factor from human plasma for structural analysis. *Hypertension* **1991**, *17*, 923–929. [[CrossRef](#)]
39. el-Masri, M.A.; Clark, B.J.; Qazzaz, H.M.; Valdes, R., Jr. Human adrenal cells in culture produce both ouabain-like and dihydroouabain-like factors. *Clin. Chem.* **2002**, *48*, 1720–1730.
40. Laredo, J.; Hamilton, B.P.; Hamlyn, J.M. Secretion of endogenous ouabain from bovine adrenocortical cells: Role of the zona glomerulosa and zona fasciculata. *Biochem. Biophys. Res. Commun.* **1995**, *212*, 487–493. [[CrossRef](#)]
41. Doris, P.A.; Hayward-Lester, A.; Bourne, D.; Stocco, D.M. Ouabain production by cultured adrenal cells. *Endocrinology* **1996**, *137*, 533–539. [[CrossRef](#)] [[PubMed](#)]
42. Qazzaz, H.M.; Cao, Z.; Bolanowski, D.D.; Clark, B.J.; Valdes, R., Jr. De novo biosynthesis and radiolabeling of mammalian digitalis-like factors. *Clin. Chem.* **2004**, *50*, 612–620. [[CrossRef](#)]
43. Bauer, N.; Muller-Ehmsen, J.; Kramer, U.; Hambarchian, N.; Zobel, C.; Schwinger, R.H.; Neu, H.; Kirch, U.; Grunbaum, E.G.; Schoner, W. Ouabain-like compound changes rapidly on physical exercise in humans and dogs: Effects of beta-blockade and angiotensin-converting enzyme inhibition. *Hypertension* **2005**, *45*, 1024–1028. [[CrossRef](#)] [[PubMed](#)]
44. Fedorova, O.V.; Lakatta, E.G.; Bagrov, A.Y. Endogenous Na,K pump ligands are differentially regulated during acute NaCl loading of Dahl rats. *Circulation* **2000**, *102*, 3009–3014. [[CrossRef](#)]
45. Fedorova, O.V.; Kolodkin, N.I.; Agalakova, N.I.; Namikas, A.R.; Bzhelyansky, A.; St-Louis, J.; Lakatta, E.G.; Bagrov, A.Y. Antibody to marinobufagenin lowers blood pressure in pregnant rats on a high NaCl intake. *J. Hypertens.* **2005**, *23*, 835–842. [[CrossRef](#)]
46. Fedorova, O.V.; Agalakova, N.I.; Talan, M.I.; Lakatta, E.G.; Bagrov, A.Y. Brain ouabain stimulates peripheral marinobufagenin via angiotensin II signaling in NaCl-loaded Dahl-S rats. *J. Hypertens.* **2005**, *23*, 1515–1523. [[CrossRef](#)]
47. Gottlieb, S.S.; Rogowski, A.C.; Weinberg, M.; Krichten, C.M.; Hamilton, B.P.; Hamlyn, J.M. Elevated concentrations of endogenous ouabain in patients with congestive heart failure. *Circulation* **1992**, *86*, 420–425. [[CrossRef](#)]
48. Manunta, P.; Ferrandi, M.; Bianchi, G.; Hamlyn, J.M. Endogenous ouabain in cardiovascular function and disease. *J. Hypertens.* **2009**, *27*, 9–18. [[CrossRef](#)]
49. Rincon-Heredia, R.; Flores-Benitez, D.; Flores-Maldonado, C.; Bonilla-Delgado, J.; Garcia-Hernandez, V.; Verdejo-Torres, O.; Castillo, A.M.; Larre, I.; Poot-Hernandez, A.C.; Franco, M.; et al. Ouabain induces endocytosis and degradation of tight junction proteins through ERK1/2-dependent pathways. *Exp. Cell Res.* **2014**, *320*, 108–118. [[CrossRef](#)] [[PubMed](#)]
50. Ponce, A.; Larre, I.; Castillo, A.; Garcia-Villegas, R.; Romero, A.; Flores-Maldonado, C.; Martinez-Rendon, J.; Contreras, R.G.; Cereijido, M. Ouabain increases gap junctional communication in epithelial cells. *Cell. Physiol. Biochem.* **2014**, *34*, 2081–2090. [[CrossRef](#)] [[PubMed](#)]
51. Vagin, O.; Turdikulova, S.; Sachs, G. Recombinant addition of N-glycosylation sites to the basolateral Na,K-ATPase beta1 subunit results in its clustering in caveolae and apical sorting in hgt-1 cells. *J. Biol. Chem.* **2005**, *280*, 43159–43167. [[CrossRef](#)] [[PubMed](#)]

52. Juliano, R.L. Adhesion and detachment characteristics of chinese hamster cell membrane mutants. *J. Cell Biol.* **1978**, *76*, 43–49. [[CrossRef](#)] [[PubMed](#)]
53. Harper, P.A.; Juliano, R.L. Isolation and characterization of chinese hamster ovary cell variants defective in adhesion to fibronectin-coated collagen. *J. Cell Biol.* **1980**, *87*, 755–763. [[CrossRef](#)] [[PubMed](#)]
54. Tokhtaeva, E.; Sun, H.; Deiss-Yehiely, N.; Wen, Y.; Soni, P.N.; Gabrielli, N.M.; Marcus, E.A.; Ridge, K.M.; Sachs, G.; Vazquez-Levin, M.; et al. The o-glycosylated ectodomain of fxyd5 impairs adhesion by disrupting cell-cell trans-dimerization of Na,K-atpase beta1 subunits. *J. Cell Sci.* **2016**, *129*, 2394–2406. [[CrossRef](#)]
55. Wang, H.; Haas, M.; Liang, M.; Cai, T.; Tian, J.; Li, S.; Xie, Z. Ouabain assembles signaling cascades through the caveolar Na<sup>+</sup>/K<sup>+</sup>-atpase. *J. Biol. Chem.* **2004**, *279*, 17250–17259. [[CrossRef](#)] [[PubMed](#)]
56. Rocha, S.C.; Pessoa, M.T.; Neves, L.D.; Alves, S.L.; Silva, L.M.; Santos, H.L.; Oliveira, S.M.; Taranto, A.G.; Comar, M.; Gomes, I.V.; et al. 21-benzylidene digoxin: A proapoptotic cardenolide of cancer cells that up-regulates Na,K-atpase and epithelial tight junctions. *PLoS ONE* **2014**, *9*, e108776. [[CrossRef](#)] [[PubMed](#)]
57. Contreras, R.G.; Shoshani, L.; Flores-Maldonado, C.; Lazaro, A.; Cerejido, M. Relationship between Na<sup>+</sup>,K<sup>+</sup>-atpase and cell attachment. *J. Cell Sci.* **1999**, *112*, 4223–4232.
58. Xie, Z. Molecular mechanisms of Na/K-atpase-mediated signal transduction. *Ann. N. Y. Acad. Sci.* **2003**, *986*, 497–503. [[CrossRef](#)]
59. Ponce, A.; Larre, I.; Castillo, A.; Flores-Maldonado, C.; Verdejo-Torres, O.; Contreras, R.G.; Cerejido, M. Ouabain modulates the distribution of connexin 43 in epithelial cells. *Cell. Physiol. Biochem.* **2016**, *39*, 1329–1338. [[CrossRef](#)]
60. Zhang, B.; Luo, Q.; Sun, J.; Xu, B.; Ju, Y.; Yang, L.; Song, G. Mgf enhances tenocyte invasion through mmp-2 activity via the fak-erk1/2 pathway. *Wound Repair Regen.* **2015**, *23*, 394–402. [[CrossRef](#)]
61. Li, W.; Liu, Z.; Zhao, C.; Zhai, L. Binding of mmp-9-degraded fibronectin to beta6 integrin promotes invasion via the fak-src-related erk1/2 and pi3k/akt/smad-1/5/8 pathways in breast cancer. *Oncol. Rep.* **2015**, *34*, 1345–1352. [[CrossRef](#)]
62. Chang, H.; Dong, T.; Ma, X.; Zhang, T.; Chen, Z.; Yang, Z.; Zhang, Y. Spondin 1 promotes metastatic progression through fak and src dependent pathway in human osteosarcoma. *Biochem. Biophys. Res. Commun.* **2015**, *464*, 45–50. [[CrossRef](#)]
63. Patel, A.; Sabbineni, H.; Clarke, A.; Somanath, P.R. Novel roles of src in cancer cell epithelial-to-mesenchymal transition, vascular permeability, microinvasion and metastasis. *Life Sci.* **2016**, *157*, 52–61. [[CrossRef](#)]
64. Flores-Benitez, D.; Rincon-Heredia, R.; Razgado, L.F.; Larre, I.; Cerejido, M.; Contreras, R.G. Control of tight junctional sealing: Roles of epidermal growth factor and prostaglandin e2. *Am. J. Physiol. Cell Physiol.* **2009**, *297*, C611–C620. [[CrossRef](#)]
65. Garcia-Hernandez, V.; Flores-Maldonado, C.; Rincon-Heredia, R.; Verdejo-Torres, O.; Bonilla-Delgado, J.; Meneses-Morales, I.; Gariglio, P.; Contreras, R.G. Egf regulates claudin-2 and -4 expression through src and stat3 in mdck cells. *J. Cell Physiol.* **2015**, *230*, 105–115. [[CrossRef](#)]
66. Haas, M.; Wang, H.; Tian, J.; Xie, Z. Src-mediated inter-receptor cross-talk between the Na<sup>+</sup>/K<sup>+</sup>-atpase and the epidermal growth factor receptor relays the signal from ouabain to mitogen-activated protein kinases. *J. Biol. Chem.* **2002**, *277*, 18694–18702. [[CrossRef](#)]
67. Li, Z.; Cai, T.; Tian, J.; Xie, J.X.; Zhao, X.; Liu, L.; Shapiro, J.I.; Xie, Z. Naktide, a Na/K-atpase-derived peptide src inhibitor, antagonizes ouabain-activated signal transduction in cultured cells. *J. Biol. Chem.* **2009**, *284*, 21066–21076. [[CrossRef](#)]
68. McNeill, H.; Ozawa, M.; Kemler, R.; Nelson, W.J. Novel function of the cell adhesion molecule uvomorulin as an inducer of cell surface polarity. *Cell* **1990**, *62*, 309–316. [[CrossRef](#)]
69. Cerejido, M.; Stefani, E.; Palomo, A.M. Occluding junctions in a cultured transporting epithelium: Structural and functional heterogeneity. *J. Membr. Biol.* **1980**, *53*, 19–32. [[CrossRef](#)]
70. Antolović, R. Low nanomolar concentrations of ouabain may induce higher activity of the Na<sup>+</sup>/K<sup>+</sup>-atpase in human erythrocytes. *Veterinarski Arhiv* **2006**, *76*, 489–495.
71. Oselkin, M.; Tian, D.; Bergold, P.J. Low-dose cardiotonic steroids increase sodium-potassium atpase activity that protects hippocampal slice cultures from experimental ischemia. *Neurosci. Lett.* **2010**, *473*, 67–71. [[CrossRef](#)] [[PubMed](#)]
72. Klimanova, E.A.; Petrushanko, I.Y.; Mitkevich, V.A.; Anashkina, A.A.; Orlov, S.N.; Makarov, A.A.; Lopina, O.D. Binding of ouabain and marinobufagenin leads to different structural changes in Na,K-atpase and depends on the enzyme conformation. *FEBS Lett.* **2015**, *589*, 2668–2674. [[CrossRef](#)]

73. Dempski, R.E.; Hartung, K.; Friedrich, T.; Bamberg, E. Fluorometric measurements of intermolecular distances between the alpha- and beta-subunits of the Na<sup>+</sup>/K<sup>+</sup>-atpase. *J. Biol. Chem.* **2006**, *281*, 36338–36346. [[CrossRef](#)] [[PubMed](#)]
74. Aperia, A.; Akkuratov, E.E.; Fontana, J.M.; Brismar, H. Na<sup>+</sup>-K<sup>+</sup>-atpase, a new class of plasma membrane receptors. *Am. J. Physiol. Cell Physiol.* **2016**, *310*, C491–C495. [[CrossRef](#)] [[PubMed](#)]
75. Khalaf, F.K.; Dube, P.; Mohamed, A.; Tian, J.; Malhotra, D.; Haller, S.T.; Kennedy, D.J. Cardiotonic steroids and the sodium trade balance: New insights into trade-off mechanisms mediated by the Na<sup>+</sup>/K<sup>+</sup>-atpase. *Int. J. Mol. Sci.* **2018**, *19*, 2576. [[CrossRef](#)] [[PubMed](#)]
76. Rajasekaran, S.A.; Gopal, J.; Willis, D.; Espineda, C.; Twiss, J.L.; Rajasekaran, A.K. Na,K-atpase beta1-subunit increases the translation efficiency of the alpha1-subunit in msv-mdck cells. *Mol. Biol. Cell* **2004**, *15*, 3224–3232. [[CrossRef](#)] [[PubMed](#)]
77. Caplan, M.J.; Anderson, H.C.; Palade, G.E.; Jamieson, J.D. Intracellular sorting and polarized cell surface delivery of (Na<sup>+</sup>,K<sup>+</sup>)atpase, an endogenous component of mdck cell basolateral plasma membranes. *Cell* **1986**, *46*, 623–631. [[CrossRef](#)]
78. Zulian, A.; Linde, C.I.; Pulina, M.V.; Baryshnikov, S.G.; Papparella, I.; Hamlyn, J.M.; Golovina, V.A. Activation of c-src underlies the differential effects of ouabain and digoxin on Ca<sup>2+</sup> signaling in arterial smooth muscle cells. *Am. J. Physiol. Cell Physiol.* **2013**, *304*, C324–C333. [[CrossRef](#)]
79. Wu, J.; Akkuratov, E.E.; Bai, Y.; Gaskill, C.M.; Askari, A.; Liu, L. Cell signaling associated with Na<sup>+</sup>/K<sup>+</sup>-atpase: Activation of phosphatidylinositide 3-kinase ia/akt by ouabain is independent of src. *Biochemistry* **2013**, *52*, 9059–9067. [[CrossRef](#)]
80. Feng, W.; Webb, P.; Nguyen, P.; Liu, X.; Li, J.; Karin, M.; Kushner, P.J. Potentiation of estrogen receptor activation function 1 (af-1) by src/jnk through a serine 118-independent pathway. *Mol. Endocrinol.* **2001**, *15*, 32–45. [[CrossRef](#)]
81. Madan, N.; Xu, Y.; Duan, Q.; Banerjee, M.; Larre, I.; Pierre, S.V.; Xie, Z. Src-independent erk signaling through the rat alpha3 isoform of Na/K-atpase. *Am. J. Physiol. Cell Physiol.* **2017**, *312*, C222–C232. [[CrossRef](#)] [[PubMed](#)]
82. Hong, S.; Troyanovsky, R.B.; Troyanovsky, S.M. Spontaneous assembly and active disassembly balance adherens junction homeostasis. *Proc. Natl. Acad. Sci. USA* **2010**, *107*, 3528–3533. [[CrossRef](#)] [[PubMed](#)]
83. Hamrick, M.; Renaud, K.J.; Fambrough, D.M. Assembly of the extracellular domain of the Na,K-atpase beta subunit with the alpha subunit. Analysis of beta subunit chimeras and carboxyl-terminal deletions. *J. Biol. Chem.* **1993**, *268*, 24367–24373.
84. Schindelin, J.; Arganda-Carreras, I.; Frise, E.; Kaynig, V.; Longair, M.; Pietzsch, T.; Preibisch, S.; Rueden, C.; Saalfeld, S.; Schmid, B.; et al. Fiji: An open-source platform for biological-image analysis. *Nat. Methods* **2012**, *9*, 676–682. [[CrossRef](#)] [[PubMed](#)]
85. Ieggli, C.V.; Bohrer, D.; do Nascimento, P.C.; de Carvalho, L.M.; Garcia, S.C. Determination of sodium, potassium, calcium, magnesium, zinc, and iron in emulsified egg samples by flame atomic absorption spectrometry. *Talanta* **2010**, *80*, 1282–1286. [[CrossRef](#)] [[PubMed](#)]
86. Paskavitz, A.L.; Quintana, J.; Cangussu, D.; Tavera-Montanez, C.; Xiao, Y.; Ortiz-Miranda, S.; Navea, J.G.; Padilla-Benavides, T. Differential expression of zinc transporters accompanies the differentiation of c2c12 myoblasts. *J. Trace Elem. Med. Biol.* **2018**, *49*, 27–34. [[CrossRef](#)] [[PubMed](#)]
87. Gordon, S.J.; Xiao, Y.; Paskavitz, A.L.; Navarro-Tito, N.; Navea, J.G.; Padilla-Benavides, T. Atomic absorbance spectroscopy to measure intracellular zinc pools in mammalian cells. *J. Vis. Exp.* **2019**, e59519, in press.
88. Raimunda, D.; Padilla-Benavides, T.; Vogt, S.; Boutigny, S.; Tomkinson, K.N.; Finney, L.A.; Argüello, J.M. Periplasmic response upon disruption of transmembrane Cu transport in *Pseudomonas aeruginosa*. *Metallomics* **2013**, *5*, 144–151. [[CrossRef](#)]
89. Cheng, L.; Wang, F.; Shou, H.; Huang, F.; Zheng, L.; He, F.; Li, J.; Zhao, F.J.; Ueno, D.; Ma, J.F.; et al. Mutation in nicotianamine aminotransferase stimulated the Fe(ii) acquisition system and led to iron accumulation in rice. *Plant Physiol.* **2007**, *145*, 1647–1657. [[CrossRef](#)]

